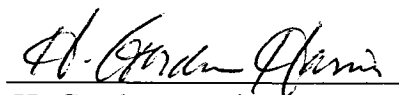
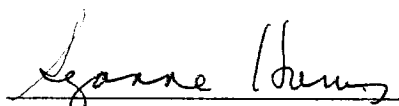


To The Graduate School:

The members of the committee approve the thesis of Xiongbo Lu presented on June 26, 2003.



H. Gordon Harris,  
Chairman

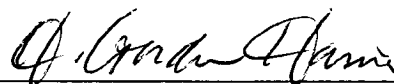


Suzanne Harris



Youqing Shen

APPROVED



H. Gordon Harris, Head, Department of Chemical Engineering



Don Roth, Dean, The Graduate School

Lu, Xiongbo, Computer Aided Process Design for Fischer-Tropsch Conversion of Coal to Liquid Fuels, M.S., Department of Chemical and Petroleum Engineering, August, 2003.

Production of synthetic liquid fuels is expected to be one of the key technologies of the twenty-first century. Coal is generally seen as the most logical feedstock for the production of synthetic fuels. Coal can be converted into liquid fuels by direct and indirect liquefaction. Among processes developed to date, Fischer-Tropsch (F-T) synthesis, in which a syngas mixture produced by coal gasification is used as a feedstock to produce higher molecular weight hydrocarbons, has received the most attention. Modern computer aided design (CAD) techniques are among the most useful tools to evaluate the various feedstocks, operating conditions, and product distributions for F-T synthesis.

In this thesis, ASPEN PLUS 11.1, one of the more complete and general software packages was used to develop a process flowsheet simulation model to evaluate the F-T conversion of coal to liquid fuels. The key aspect of this model is a user-defined module based on a single chain growth mechanism model known as the Anderson-Shultz-Flory (ASF) distribution model. This user-defined module predicts the F-T product selectivity under specific operating conditions. A base case and several cases with different operating conditions specified in F-T synthesis were then calculated to examine the effects of operating conditions on F-T product selectivity. An economic estimate on the capital investment in the conversion of coal to liquid fuels via F-T synthesis is provided.

Future work would include: refining the APEN PLUS process flowsheet simulation model to more accurately represent the conversion of coal to liquid fuels with a focus on incorporating a more accurate product distribution model into the user-defined module to more reliably predict the F-T synthesis product selectivity and developing a detailed economic analysis based on the ASPEN PLUS process flowsheet simulation model developed in this thesis for use in future F-T synthesis projects.

COMPUTER AIDED PROCESS DESIGN FOR FISCHER-TROPSCH  
CONVERSION OF COAL TO LIQUID FUELS

by  
Xiongbo Lu

A thesis submitted to the Department of Chemical and Petroleum Engineering  
and The Graduate School of The University of Wyoming  
in partial fulfillment of the requirements  
for degree of

MASTER OF SCIENCE  
in  
CHEMICAL ENGINEERING

Laramie, Wyoming  
August, 2003

UMI Number: EP22630

### INFORMATION TO USERS

The quality of this reproduction is dependent upon the quality of the copy submitted. Broken or indistinct print, colored or poor quality illustrations and photographs, print bleed-through, substandard margins, and improper alignment can adversely affect reproduction.

In the unlikely event that the author did not send a complete manuscript and there are missing pages, these will be noted. Also, if unauthorized copyright material had to be removed, a note will indicate the deletion.

**UMI**<sup>®</sup>

---

UMI Microform EP22630

Copyright 2007 by ProQuest Information and Learning Company.

All rights reserved. This microform edition is protected against unauthorized copying under Title 17, United States Code.

ProQuest Information and Learning Company  
300 North Zeeb Road  
P.O. Box 1346  
Ann Arbor, MI 48106-1346

## Contents

	Page No.
I. Introduction	1
A. World Supply and Demand of Liquid Fuels	3
B. Projection of World Supplies of Liquid Fuels	3
C. Processes for Conversion of Gases and Solids to Liquid Fuels	4
D. World Reserve of Coal and Wyoming Coal Reserves	5
II. Fischer-Tropsch Process for Conversion of Coal to Liquid Fuels	8
A. History and Industrial Development of Fischer-Tropsch Synthesis	8
B. Mechanism of Fischer-Tropsch Synthesis	9
C. Previous Experimental Studies for Fischer-Tropsch Synthesis	11
D. Comparison of Predicted and Experimental Results of Fischer-Tropsch Synthesis	13
III. Introduction and Description of ASPEN PLUS CAD Software	27
IV. Process Flowsheet Model Description	29
A. Individual Plant Components of Section 1: Syngas Generation and Preparation Processes	30
1. Plant 101 Coal Drying Plant	
2. Plant 102 Shell Gasification Plant	
3. Plant 103 Syngas Cooling & Cleanup Plant	
B. Individual Plant Components of Section 2: Fischer-Tropsch Synthesis and Product Recovery	33
1. Plant 201 CO Shift Plant	
2. Plant 202 Fischer-Tropsch Synthesis Plant	
3. Plant 203 Hydrocarbon Products Recovery Plant	
V. Results of Process Flowsheet Simulation	40
A. Case I – Base Case	40
B. Case II – Catalyst Effect	43
C. Case III – Temperature Effect	44
D. Case IV – Pressure Effect	45

	Page No.
VI. Economics	47
VII. Discussion	48
VIII. Conclusions and Recommendations for Future Work	50
A. Conclusions	50
B. Recommendations for Future Work	51
IX. References	52
X. Appendices	55
A. Input File Listing of the ASPEN PLUS Process Flowsheet Simulation Model of Section 1-Base Case	55
B. Input File Listing of the ASPEN PLUS Process Flowsheet Simulation Model of Section 2 - Base Case	61
C. MS Excel Spreadsheets Incorporated in the User-defined Model (P202FT) - Base Case	74

## Tables

<u>Table</u> <u>No.</u>	<u>Title</u>	<u>Page</u> <u>No.</u>
1.	World Fuels Supply and Demand 1996-2020	4
2.	Wyoming Coal Production and Number of Mines in 1978 and 1997	7
3.	Carbon Number Distribution in Classical F-T Synthesis	15
4.	Properties of the Feeds to Plant 201	31
5.	Physical Properties of Raw Coal	31
6.	Typical Gas Composition After Shell Gasification Process	40
7.	Output of Plant 102 (Stream 102S3 and Stream ASH)	41
8.	Output of Plant 103 (Stream 103S5)	41
9.	Output of Plant 201 (Stream 201S6)	42
10.	Base Case Simulation Results – Properties of the Products	42
11.	Base Case Simulation Results - Product Selectivity	43
12.	Simulation Results of Catalysts' Effect on Product Amount	43
13.	Simulation Results of Catalysts' Effect on Product Selectivity	44
14.	Simulation Results of Temperature' Effect on Product Selectivity	44
15.	Simulation Results of Temperature' Effect on Amount of C <sub>5+</sub> Products and Conversion Efficiency	44
16.	Simulation Results of Pressure's Effect on Product Selectivity	45
17.	Simulation Results of Pressure's Effect on Amount of C <sub>5+</sub> Products and Conversion Efficiency	46
18.	Estimated Fixed Capital Investments	47

## Figures

<u>Figure</u> <u>No.</u>	<u>Title</u>	<u>Page</u> <u>No.</u>
1.	Oil Supply Profiles of 1996-2030	3
2.	Coal Rank	6
3.	Product Distribution of F-T Synthesis Over Co Catalyst	15
4.	Typical Carbon Number Distribution of Co, Fe, and Ru Catalysts	16
5.	Experimental Data and Simulation Results of Co Catalysts -1	17
6.	Experimental Data and Simulation Results of Co Catalysts -2	18
7.	Experimental Data and Simulation Results of Co Catalysts -3	18
8.	Experimental Data and Simulation Results of Ni Catalysts	19
9.	Experimental Data and Simulation Results of Fe Catalysts	20
10.	Experimental Data and Simulation Results of Ru Catalysts	20
11.	SASOL Synthol Plant Data and Simulation Results	21
12.	SASOL Arge Plant Data and Simulation Results	22
13.	Rheinprussen Plant Data and Simulation Results	22
14.	Mobile Plant Data Simulation Results	23
15.	Satterfield's Data of Ruhrchemie Catalyst and Simulation Results	23
16.	Satterfield's Data of C-73 Catalyst and Simulation Results	24
17.	ASPEN PLUS Flowsheet of Plant 101 and Plant 102	30
18.	ASPEN PLUS Flowsheet of Plant 103	32
19.	ASPEN PLUS Flowsheet of Plant 201	33
20.	ASPEN PLUS Flowsheet of Plant 202	34
21.	ASPEN PLUS Flowsheet of Plant 203	38



## I. INTRODUCTION

As worldwide demand for energy increases, conventional crude oil reserves are expected to be substantially depleted within the next few decades. To maintain an adequate liquid fuel supply, production of synthetic liquid fuels is one of the key technologies of the twenty-first century.

Coal reserves are abundant, and coal is generally seen as the most logical feedstock now under consideration for the production of synthetic fuels. Coal can be converted into liquid fuels by direct and indirect liquefaction. Among processes developed to date, Fischer-Tropsch (F-T) synthesis, in which a syngas mixture produced by coal gasification is used as a feedstock to produce higher molecular weight hydrocarbons over a metallic catalyst, has received the most attention. Modern computer aided design (CAD) techniques are among the most useful tools to evaluate the various feedstocks, operating conditions, catalysts, and product distributions for F-T synthesis. A variety of CAD software packages have been developed for design and analysis of chemical processes. In this thesis, ASPEN PLUS 11.1, one of the more complete and general packages is used to evaluate F-T conversion of coal to liquid fuels.

Many of the steps in Fischer-Tropsch conversion of coal to liquids process involve conventional chemical engineering processes, and simulation of such processes is comparatively straightforward. For example, to represent the coal gasification process, a RGIBBS reactor block of ASPEN PLUS simulates syngas generation employing feed of dry coal and oxygen. The RGIBBS function minimizes the Gibbs free energy of the products from coal gasification, and thus is able to calculate product distribution assuming chemical equilibrium is achieved. Another example is the use of an ASPEN PLUS REQUIL reactor block to represent the CO shift process; in this step hydrogen production in a water-gas shift reactor is assumed to be in thermodynamic equilibrium. Both of these equilibrium calculations yield product distributions close to equilibrium. In fact, most of the unit operations in F-T synthesis can be closely approximated via the ASPEN PLUS block models, and a complete simulation of these processes has been completed and is described in the following chapters.

However, ASPEN PLUS does not have a subroutine or reactor block which can be used to calculate the product distribution or selectivity of the F-T products. To overcome this problem, user-defined model is necessary to calculate the product selectivity of F-T synthesis and predict liquid products distribution.

One of the primary goals of this thesis is development of a user-defined module in the ASPEN PLUS CAD package that will reliably calculate liquid product distribution for F-T synthesis reactions.

In this thesis, an exhaustive literature search identified thirteen experimental studies that reported product distributions from F-T synthesis. A number of schemes have been suggested for analyzing and interpreting F-T reaction product distributions. The hydrocarbon chain growth probability model of predicting F-T product selectivity has been the most successful. Several types of chain growth models, using different numbers of chain growth probabilities, have been developed to characterize the F-T product distribution. The analysis of the thirteen studies available showed a single chain growth probability model, the Anderson-Schultz-Flory (ASF) distribution model, closely predicted the F-T product distribution. Consequently, to simplify the calculations, the user-defined model in the ASPEN PLUS flowsheet simulation uses the ASF single chain growth probability model. A Microsoft Excel spreadsheet, incorporated into the user-defined model, calculates product distributions.

The remainder of Chapter I discusses current and future world liquid fuels supply and demand, introduces processes of utilizing alternative energy sources, especially coal reserves, as the feedstock of synthetic liquid fuels, and discusses the world and Wyoming coal reserves.

Chapter II introduces the history and mechanism of Fischer-Tropsch synthesis. Reported experimental results for product distribution of Fischer-Tropsch synthesis of previous studies are analyzed using the Anderson-Schultz-Flory distribution model.

Chapter III introduces ASPEN PLUS CAD software and describes the steps of setting up a process flowsheet simulation.

Chapter IV describes the ASPEN PLUS process flowsheet simulation model for the coal to liquid fuels process via F-T synthesis and simulation models for six major plants.

Chapter V presents the results of the simulation of a base case as well as calculations of several cases with different operating conditions specified in F-T synthesis to examine the effects of operating conditions on F-T product selectivity.

Chapter VI provides an economic estimate of the total capital investment of the F-T conversion of coal to liquid fuels process.

Chapter VII and Chapter VIII present discussion and conclusions and recommend future work.

## A. World Supply and Demand of Liquid Fuels

The world economy is still heavily dependent on petroleum despite considerable efforts that have been devoted to the development and exploitation of alternative energy. Petroleum accounts for approximately 40% of the world's total energy consumption, down by only 8% from the energy crisis of 1973. Absolute petroleum consumption has increased by 50% during the same time period. Although proved recoverable reserves of petroleum rose 60% between 1973 and 1993, many studies have shown that the world petroleum reserve will be mostly depleted within about 30 years. Table 1 [1] provides projections for supply and demand of liquid fuels.

Table 1. World Fuels Supply and Demand 1996-2020: Historic and Projected Assuming a Lower Estimate of Conventional Oil Reserves - 2.3 Trillion Barrels (In million barrels per day)

Year	1996	2000	2010	2020
Total demand for liquid fuels	72.0	78.3	94.5	110.1
Total natural gas liquids, processing gains, and identified unconventional oil	9.3	11.6	15.5	20.6
Conventional crude oil				
Middle East OPEC	17.2	20.1	40.9	45.2
World excluding Middle East OPEC	45.5	46.6	38.0	27.0
Total crude oil	62.7	66.7	78.9	72.2
World liquids supply excluding unidentified unconventional oil	72.0	78.3	94.5	92.8
Balancing item - unidentified unconventional oil	0.0	0.0	0.0	17.3

The world total production of crude oil, the main source of liquid fuels, reached 66.7 million barrels per day in 2000. However, the world demand of liquid fuels exceeded supply by 11.6 million barrels per day. Production of unconventional fuels, produced by various synthesis processes, fills the gap between the liquid fuels demand and crude oil supply.

## B. Projection of World Supplies of Liquid Fuels

The International Energy Agency (IEA) prepared an analysis of the prospects for oil production by region, paying particular attention to the distinction between OPEC Middle East and all other producers. The agency accounted estimates of conventional oil reserves and the production profiles for oil in each region.

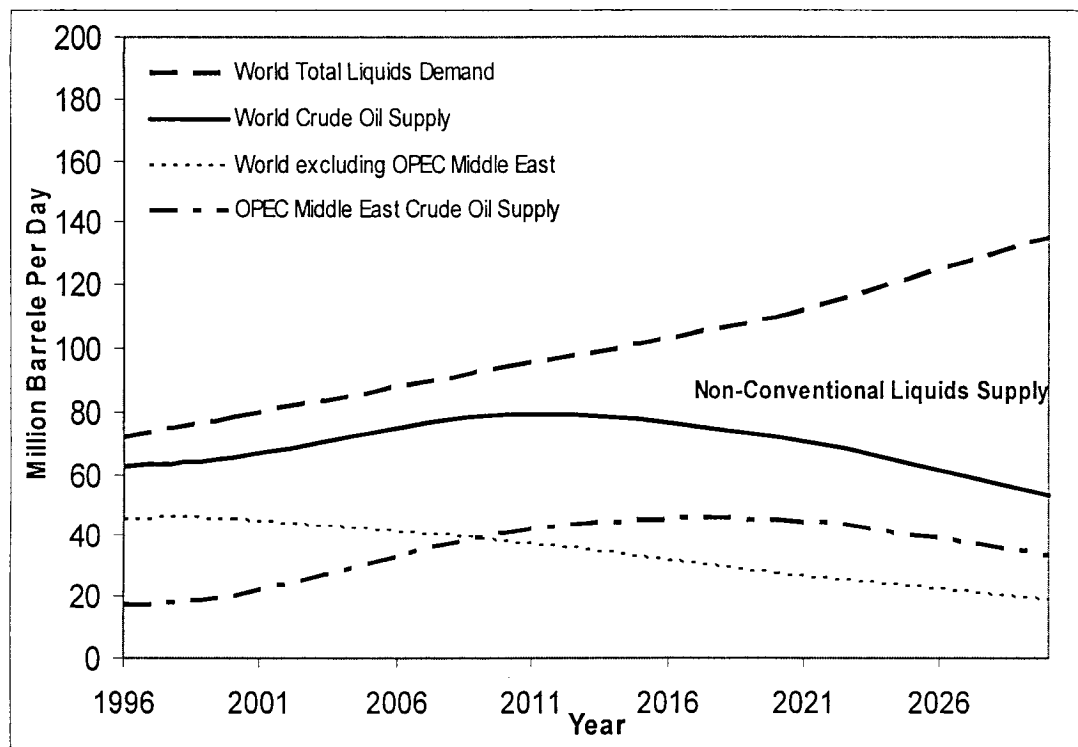


Figure 1. Oil Supply Profiles of 1996-2030

Figure 1 shows Business-As-Usual (BAU) [1] projections of oil production profiles, assuming ultimate recoverable reserves of conventional oil of 2.3 trillion barrels, for the world, OPEC Middle East, and all other areas. World demand for liquid fuels was projected to 2030 using the average growth rate of 1995-2020 to highlight the longer-term oil supply picture. Table 1 gives details of prospective supplies for conventional and non-conventional oil to the year 2020. The transition from conventional to non-conventional oil as the marginal supply in 2015 is assumed to raise the oil price over the period from 2010 to 2015. The use of non-conventional oil expands rapidly after 2015 as it meets the increase in demand for liquid fuels and compensates for the decline in conventional oil production. To produce large and increasing volumes of oil from non-conventional sources will require many major multi-billion dollar projects. Some unevenness in supply availability is possible because of the long lead times required for these big projects and the difficulties in matching supply to demand.

### C. Processes for Conversion of Gas and Solid to Liquid Fuels

With world-wide increasing demand for energy, many projections indicate conventional crude oil reserves are expected to be mostly depleted within the next few decades. Alternative feedstock utilization is thus one of the key technologies

of the twenty-first century for maintaining an adequate world energy supply. Natural gas, coal, oil shale, tar sand, and wood can be converted into liquid fuels by various processes. Natural gas and coal are the most common sources for conversion into synthetic fuels to make up the shortfall in liquid fuels.

Several technologies for conversion of natural gas to liquid transportation fuels have been developed, such as the Gulf-Badger process, Selective Oxidation (SELOX) process, and Shell Middle Distillate Synthesis (SMDS) process. Some are now available for commercial application. All involve the conversion of natural gas into syngas. Further processing involves the Fischer-Tropsch synthesis, methanol synthesis, or dimethyl ether (DME) synthesis. These technologies are capable of standing alone or can be judiciously combined.

Coal is generally seen as the most logical source for the production of synthetic fuels. Coal can be converted into liquid fuels by direct and indirect liquefaction. There are five major processes for coal conversion: EDS (Exxon Donor Solvent), H-Coal (developed by Hydrocarbon Research, Inc.), SRC (Solvent Refined Coal), MTG (Mobile Methanol-to-Gasoline), and Fischer-Tropsch (F-T) synthesis. The first three processes are direct coal liquefaction and the other two are indirect coal liquefaction, producing liquid fuels from coal-derived synthesis gas. Among those five processes, the F-T synthesis has received the most attention.

#### **D. World Reserve of Coal and Wyoming Coal Reserves**

The proven world coal reserve base is 1,011 billion tons. This includes anthracite, bituminous, subbituminous, and lignite qualities. Coal has maintained its long-term position as the world's most widely available fossil fuel, ahead of oil and natural gas. Current annual production totals 4.7 billion tons in 72 countries around the world. At current production rates, present reserves would support demand for over 200 years.

Coal is generally expected to continue supplying a large portion of the world's primary energy demand, especially in developing nations such as India and China. The future of both the production and use of coal depends to a large degree on technical progress. Mining techniques and upgrading processes must be improved.

Coal usually is divided into two main classes: anthracite (hard coal) and bituminous (soft coal). Anthracite is the highest ranking coal and contains the highest percentage of carbon and the lowest percentage of moisture. Anthracite makes up only a small part of the world's supply of coal. About half of the world's coal reserve is bituminous coal. Remaining coal reserves are even softer (sub-

bituminous and lignite). Figure 2 shows the relative rank of different classes of coal. [2]

Moisture decreases, rank increases.  
 Rank increases, fixed carbon increases.  
 Rank increases, volatile matter decreases.  
 Rank increases, heating value increases (optimum Btu at low-volatile bituminous).

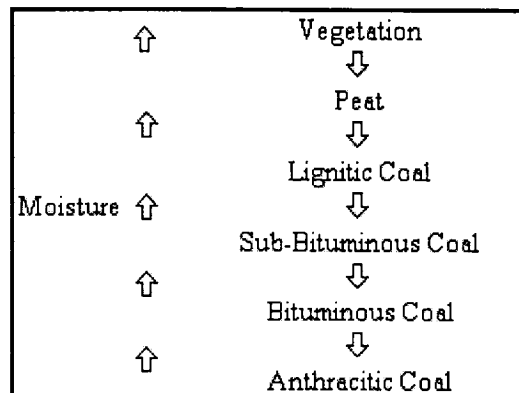


Figure 2. Coal Rank

About 90% of the United States' coal reserves are concentrated in 10 states. Montana, Illinois, Wyoming, West Virginia, and Kentucky top the list of states with the most coal. Montana ranks No. 1, with 25% of known coal reserves that could be profitably mined and marketed. Wyoming, ranking third in coal supply, is first in coal production, accounting for 18 % of annual production.

Coal was discovered in Wyoming before 1834 on the Bell Fourche River. The state's first mine opened in Carbon County in 1865, and with the completion of the transcontinental railroad, the demand for coal increased. In 1987, Wyoming became the largest coal-producing state in the country. The state is known for its extensive coal resources and extremely thick coal seams. Wyoming's coal reserves total about 69.3 billion tons, 14.2 % of the U.S. coal reserve. Coal seams range generally from 10 to 80 feet in thickness. The coal bearing areas of Wyoming underlie about 41% of the State's total land area. Wyoming's coal ranks from lignite to highly volatile bituminous. Most of the coal produced, from the Powder River coal region near Gillette, is subbituminous. Currently approximately 80 % of Wyoming's coal production is shipped out of state to meet the growing demand for low-sulfur coal to fuel electric generating plants. Table 2 [3] gives Wyoming coal production and the number of coal mines in 1978 and 1997.

Table 2. Wyoming Coal Production and Number of Mines in 1978 and 1997

Tons Produced (tons)	1978		1997	
	Amount	Percent of U.S. Total	Amount	Percent of U.S. Total
Surface	40,057,387	16.4%	279,136,734	48.1%
Underground	518,395	0.3%	2,400,488	0.5%
Lignite	0	0%	0	0%
<b>Total</b>	<b>40,575,783</b>	<b>9.7%</b>	<b>281,537,222</b>	<b>25.9%</b>
<b>Number of Producing Mines</b>				
Surface (bituminous coal)	24	0.7%	34	1.4%
Underground	2	0.07%	3	0.1%
Lignite (surface)	0	0%	0	0%
<b>Total</b>	<b>26</b>	<b>0.4%</b>	<b>37</b>	<b>0.8%</b>

Wyoming offers great potential for the establishment of commercial plants to convert coal to liquid fuels. Such plants would greatly enhance the economic activity within Wyoming.



## II. F-T PROCESS FOR CONVERSION OF COAL TO LIQUID FUELS

Coal is generally considered the most logical conventional feedstock for the production of synthetic liquid fuels. Coal conversion technology has been understood for quite some time and was used in Germany during World War II to produce large quantities of transportation fuels. Presently, South Africa produces liquid fuels by their SASOL F-T Synthesis processes to supply the majority of their fuel demand.

### A. History and Industrial Development of Fischer-Tropsch Synthesis

Gasoline and other liquid fuels can be obtained from coal by indirect hydrogenation, known as the Fischer-Tropsch synthesis process. Franz Fischer and Hans Tropsch invented F-T synthesis in the 1920's in Germany. Coal, lignite, or natural gas is first converted into "water gas," a mixture of CO and H<sub>2</sub> also known as "syngas". After purification, the mixture of gases with the proper ratio of CO and H<sub>2</sub> then goes through a solid catalyst to produce gasoline, diesel oil, paraffin wax, and alcohols.

Catalytic hydrogenation of CO has been actively studied for a century. In 1902, P. Sabatier and J.D. Senderens hydrogenated CO over Ni to produce CH<sub>4</sub> at a temperature between 200°C and 250°C. In 1913, Badische Anilin und Soda Fabrik (BASF) received patents on the preparation of hydrocarbons and oxygenates by the hydrogenation of CO at high pressure, usually on oxide catalysts, such as oxides of cobalt, osmium, or zinc. In 1923, Fischer and Tropsch obtained Synthol, mostly oxygenates from H<sub>2</sub> and CO on alkaliized Fe and other catalysts. In 1925, Fischer and Tropsch announced the synthesis of high hydrocarbons at atmospheric pressure on Co and Ni catalysts. They found olefins and saturated paraffins with boiling points between 60°C and 185°C during their work. From 1926 to 1930, studies were made on the new process in England, Japan, and the United States.

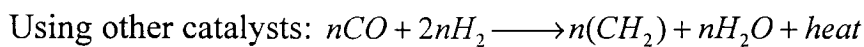
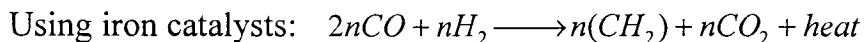
By 1932, Fischer and K. Meyers developed some new Ni and Co catalysts, which greatly improved the yield of the liquid hydrocarbons, by better methods of preparation. Because their process succeeded on a laboratory scale, they recommended pilot-plant experimentation. In 1933, the Ruhrchemie A.G. undertook the pilot-plant tests using Ni catalyst and made further progress on Co catalysts. From 1935 to 1945, several commercial plants were built in Ruhr, Germany, using coke from bituminous coal as the source of synthesis gas to produce gasoline, kerosene, and diesel oils. In 1937, Fischer and Pichler discovered that synthesis on Fe was greatly improved at 5 to 20 atm. The alkaliized Fe catalyst in this pressure range became a possible replacement for the Co catalyst in the German commercial plants.



After World War II, new progress was made on Fischer-Tropsch synthesis. In 1950, a fluidized-fixed bed process developed by Hydrocarbon Research, Trenton, New Jersey, was installed in Brownsville, Texas. This plant, called Carthage Hydrocol, Inc., used reformed natural gas as feed. In 1953, a new reactor was installed because there were several operating difficulties. Although the plant was operating properly, it was promptly shut down, sold, and dismantled because of the high cost of natural gas. At the same time, in South Africa, the SASOL F-T synthesis plant using coal was constructed. It opened in 1955. Lurgi gas generators and Rectisol gas-cleaning units were employed. Two types of reactors, both with Fe catalysts, were used: a fixed-bed with recycle units and an entrained-solids reactor. These units have successfully operated up to the present. In 1975, the decision was made to build a SASOL II and in 1979 plans were made for SASOL III. The new plants were similar to the initial plants, except that the fixed-bed reactors were not included in the new installations. [4]

## B. Mechanism of Fisher-Tropsch Synthesis

The main catalysts active in the Fischer-Tropsch synthesis are cobalt, iron, nickel, and ruthenium, with iron and cobalt most favored. The reactions between hydrogen and carbon monoxide to form hydrocarbons may be expressed empirically by means of the following equations:



In these formulas (CH<sub>2</sub>) represents the hydrocarbons produced. This reaction will generate about 20% of the heat of combustion of the synthesis gas. [5]

It is well known that the products of the F-T reaction cannot be closely controlled; in other words, one cannot “obtain a hydrocarbon product in which the individual molecules all have the exact  $n$  carbon numbers, nor even a product where  $n$  is constrained in some narrow range,  $a \leq n \leq b$ .” [5] So the detailed mechanism of the Fischer-Tropsch reaction remains a subject of controversy. However, there is an agreement amongst the researchers as to what happens on the catalyst surface, which is sufficient to provide a model, known as chain growth probability model that can be verified by the bulk of the experiment results. .

There are four assumptions [5] of this model:

1. Reaction is initiated on the surface by some species containing a single carbon.
2. Chain growth takes place from the initiating species by the addition of one carbon at a time.
3. Chain growth is terminated in some way, which leads to adsorption of the product molecules and creates a vacant site on the surface for further reaction.
4. The rates of the growth and termination reactions are independent of the chain growth and are of the same order in the surface concentration of the species in question.

The only parameter of the model is  $\alpha$ , the chain growth probability, which represents the probability that an oligomer with  $k-1$  carbon atoms will grow to an oligomer with  $k$  carbon atoms. The probability that chain growth up to carbon atoms  $C_{n-1}$  takes place is  $\alpha^{n-1}$ . Chain termination at carbon atoms  $C_n$  then has the probability:

$$X_n = \alpha^{n-1}(1-\alpha)$$

$X_n$  is also the mole fraction of the hydrocarbon product with carbon atoms number  $n$ . It can also be written as

$$\log X_n = n \log \alpha + \log[(1-\alpha)/\alpha]$$

Approximating the reaction by a factor of  $-\text{CH}_2-$  units (MW=14) the corresponding mass is given by

$$w_n = 14n\alpha^{n-1}(1-\alpha)$$

and the mass fraction by

$$W_n = \frac{w_n}{\sum_1^{\infty} w_n}$$

$$\sum_1^{\infty} w_n = 14(1-\alpha) \sum_1^{\infty} n\alpha^{n-1} = 14(\alpha-1) \left[ \frac{1}{1-\alpha} \right]^2 = \frac{14}{1-\alpha}$$

$$\therefore W_n = n\alpha^{n-1}(1-\alpha)^2$$

and can be written as:

$$\log(W_n/n) = n \log \alpha + \log[(1-\alpha)^2/\alpha]$$

The expression above is usually known as the Anderson-Schultz-Flory (ASF) polymerization equation. Schulz and Flory first derived it to describe

polymerization and condensation reactions, and it was later applied independently to the Fischer-Tropsch reaction by Herington, Friedel, Anderson, and others. [5] If the product distribution among the carbon numbers follows the above equation, one would expect a linear relation between  $\log(W_n/n)$  and  $n$ , with the slope of  $\log \alpha$ .

### C. Previous Experimental Studies for Fischer-Tropsch Synthesis

The key to developing an adequate CAD package for Fischer-Tropsch conversion of coal to liquid fuels is developing a reliable module to predict product distribution of the F-T synthesis. The model described in the above section, which is known as a single chain growth probability model or Anderson-Schultz-Flory (ASF) polymerization model, was verified by the bulk of the reported experiment results and is sufficient to provide a method of predicting F-T product distribution. The ASF model is applied in a Microsoft Excel spreadsheet incorporated into the user-defined model in the ASPEN PLUS process flowsheet simulation to predict the F-T product distribution.

Thirteen independent studies on Fischer-Tropsch synthesis have been reported in the literature. These studies were conducted over more than 50 years and covered laboratory work to full-scale commercial plants. These studies reported experimental data on F-T product selectivity. In the following paragraphs, each of these thirteen studies is summarized.

Study I. R.B. Anderson [10] studied the kinetics and reaction mechanism of the Fischer-Tropsch synthesis. He reviewed the carbon number distributions in classical F-T synthesis of Co and Fe catalysts and observed molar carbon-number distribution showing a linear part in a semilogarithmic plot for carbon numbers up to 20, which is the characteristic expression of the Anderson-Schultz-Flory chain growth mechanism.

Study II. Storch, Golumbic, and R.B. Anderson [11] studied Fischer-Tropsch and related synthesis and observed a linear correlation between  $\log(W_n/n)$  and carbon number  $n$  with a slope of  $\log \alpha$ , which is another expression of the ASF chain growth mechanism, over Co catalyst.

Study III. In more recent investigation by Sie [12, 13], in which a few hundred independent F-T synthesis experiments were carried out with various catalyst formulations under different operating conditions and with analytical techniques more accurate than those adopted in the past, a good fit of the observed carbon number distributions to the ASF model was observed with Fe, Ru, and Co types of

catalysts. It was found that the product distributions were indeed in close agreement with the Anderson-Shultz-Flory chain growth mechanism with  $\alpha$  value varying.

Study IV. Storch, R.B. Anderson, and their coworkers [14] carried on research on the synthetic fuels from hydrogenation of carbon monoxide for the Department of Energy. Their study contained a detailed record of experimental work done from 1943 to 1946 on the effect of the mode of catalyst preparation, reduction and induction on activity in the synthesis, and on the boiling range of the product. They conducted a series of experiments on different types of Co catalysts under a pressure of 100 psi and with a temperature range from 174°C to 208°C and on different types of Ni catalyst at atmosphere pressure and with a temperature range from 190°C to 205°C. The selectivities of the C<sub>5+</sub> products were reported in these experiments.

Study V. Chaumette [15] studied the conversion of syngas to middle distillates on modified Co catalysts. He investigated the reactivity of Co catalysts at 220°C and 20atm. He reported the selectivities of the C<sub>5+</sub> products obtained on different Co-based catalytic systems and in both a fixed bed and a slurry phase reactor.

Study VI. Udaya [16] studied the bifunctional Co catalysts in syngas conversion at 280°C and 21atm. He compared the C<sub>5+</sub> product selectivities of the bifunctional Co catalysts in a microreactor with those obtained in dual reactor studies with separated F-T and zeolitic components.

Study VII. Sethuraman [19] conducted a series of experiments to study the production of C<sub>4</sub> hydrocarbons from Fischer-Tropsch synthesis in a follow bed reactor consisting Co-Ni-ZrO<sub>2</sub> over sulfated-ZrO<sub>2</sub> catalyst beds as well as a fixed bed reactor over a single bed consisting of Co-Ni-ZrO<sub>2</sub> catalysts. He examined the temperature effect on F-T synthesis product selectivity through experiments carried out at three temperature points: 513°K, 523°K, and 533°K under low reaction pressure. The C<sub>5+</sub> product selectivities were reported.

Study VIII. Hadjigeorghiou and Richardson [17] studied F-T selectivity of coprecipitated Ni/Al<sub>2</sub>O<sub>3</sub> catalysts. They reported the C<sub>5+</sub> product selectivities in both an integral reactor and CSTR under atmosphere pressure and a temperature range from 220°C to 250°C.

Study IX. Shultz and his coworkers [18] from Department of Energy studied methods of preparation, characterization, and reaction mechanisms of Fe catalysts for the Fischer-Tropsch synthesis. They carried out several synthesis tests using differently prepared Fe catalysts under a pressure of 7.8atm and a temperature range from 220°C to 260°C and reported the selectivities of the C<sub>5+</sub> products.

Study X. Everson [20] undertook Hydrocarbon synthesis to study the Fischer-Tropsch  $C_{5+}$  selectivity on 0.5% Ruthenium-on-alumina pellets catalyst. They carried out experiments in a gas-solid reactor under a medium pressure of about 8 bars and at a temperature close to 500°K. The selectivities of the  $C_{5+}$  products were reported.

Study XI. Rao [21] reviewed the technology of Fe-based catalysts for the slurry-phase Fischer-Tropsch process. In this review, he reported SASOL plant data of Fischer-Tropsch product selectivity of an Arge reactor operating at 325°C and 25atm using fused Fe in a circulating fluidized bed reactor and a Synthol reactor operating at 220°C and 25atm using precipitated Fe catalysts in a fixed-bed reactor. He also reviews the product selectivity of a Rheinprussen demonstration plant operating at 268°C and 12atm using 100Fe/0.1Cu/0.05-0.5K<sub>2</sub>O catalyst in a bubble-column slurry reactor. The product selectivity in groups of  $C_1$ - $C_4$  (fuel gas),  $C_5$ - $C_{11}$  (naphtha),  $C_{12}$ - $C_{18}$  (distillates), and  $C_{19+}$  (wax) was reported.

Study XII. Kuo [23] studied the Mobile two-stage process of converting syngas to transportation fuel in 1983. The Mobile plant operates at 260°C and 15atm using Fe/Cu/K<sub>2</sub>O catalyst in a bubble-column slurry reactor. The product selectivity in groups of  $C_1$ - $C_4$  (fuel gas),  $C_5$ - $C_{11}$  (naphtha),  $C_{12}$ - $C_{18}$  (distillates), and  $C_{19+}$  (wax) was reported.

Study XIII. Satterfield and his coworkers [number?] at MIT studied Fischer-Tropsch synthesis activity and selectivity of the two commercial catalysts: Ruhrchemie catalysts and C-73 fused magnetic catalysts in a stirred tank slurry reactor. Srivastava [24] reviewed the results of their research on F-T product selectivity and presented it in three sections:  $C_1$ - $C_4$  (fuel gas),  $C_5$ - $C_{12}$  (naphtha), and  $C_{13+}$  (distillates and wax).

#### **D. Comparison of the Predicted and Experimental Results of Fischer-Tropsch Synthesis**

The previous experimental studies on Fischer-Tropsch product distribution were analyzed to determine if the ASF distribution model is adequate to predict the Fischer-Tropsch product selectivity. The results calculated by the ASF model in the user-defined module of the ASPEN PLUS process flowsheet simulation were compared with the experimental results to see how accurately the ASF model predicted the F-T product distribution, a main concern of the CAD design of the F-T conversion of coal into liquid fuels.

The ASF model was verified in three stages. In the first stage, the experimentally observed carbon number distributions of Fischer-Tropsch synthesis products were

compared to those predicted by the Anderson-Shultz-Flory model. In the second stage, the accuracy of the simulation model's predictions of F-T  $C_{5+}$  product selectivity was verified under various operating conditions with different types of catalysts. In the third stage of the verification process, the prediction of the simulation model of a more detailed selectivity of major F-T synthesis products groups was examined. (The major product groups are  $C_1-C_4$  (fuel gas),  $C_5-C_{11}$  (naphtha),  $C_{12}-C_{18}$  (distillates), and  $C_{19+}$  (wax) and  $C_1-C_4$ ,  $C_5-C_{12}$  and  $C_{13+}$  in the last study.) For each of these three cases, the accuracy of the simulation model was compared with experimental data.

Studies I, II, and III show that the linear relation of the ASF chain growth mechanism described in Chapter II has already been observed in the classical F-T literature. (The mechanism is used in the user-defined module in ASPEN PLUS process flowsheet simulation to predict the F-T product distribution.) Thus it is reasonable to use the ASF distribution model in the user-defined module to predict the carbon number distribution of the Fischer-Tropsch products.

The comparisons between the reported experimental results of Studies IV to X and the predicted results of the user-defined model show that the model produces reasonable predictions of  $C_{5+}$  product selectivity under different operating conditions with different types of catalysts. The  $C_{5+}$  hydrocarbons from Fischer-Tropsch synthesis are recovered and hydrotreated to produce high-value products such as gasoline and diesel fuels, while the lighter hydrocarbons are often utilized as fuel gas. The selectivity of  $C_{5+}$  products is also an important index of the catalyst activity in the F-T reaction. The  $C_{5+}$  products selectivity thus becomes a major component of F-T synthesis and must be predicted.

The comparisons between the experiments from Studies XI, XII, and XIII and the predicted results from the model show good fits of the model predictions to the experimental data of the selectivity of the major F-T product groups. The major product groups are  $C_1-C_4$  (fuel gas),  $C_5-C_{11}$  (naphtha),  $C_{12}-C_{18}$  (distillates), and  $C_{19+}$  (wax) in Study XI and XII, and  $C_1-C_4$ ,  $C_5-C_{12}$ , and  $C_{13+}$  in Study XIII.

Studies I, II, and III are the classical studies of the F-T product distribution. They show that the linear relation of the ASF chain growth mechanism used in the user-defined module in ASPEN PLUS process flowsheet simulation to predict the F-T product distribution has been observed in the bulk of classical literature of F-T synthesis.

Using data from R.B. Anderson's [10] Study I, Table 3 illustrates that the observed molar carbon-number distribution showed a linear part in a semilogarithmic plot for carbon numbers up to 20, the characteristic expression of the Anderson-Shultz-Flory chain growth mechanism.



Table 3. Carbon Number Distribution in Classical F-T Synthesis [10]

Source of Data	Range separated, Carbon number	Linear portion, Carbon number	$\alpha$
<b>Cobalt Catalysts</b>			
Ward	14-18	14-18	0.76
Herington	5-11	5-11	0.76
Gibson, Gall, Hall			
Hydrocarbons	6-11	6-11	0.75
Alcohols	4-8	4-8	0.73
Ruhrchemie			
Atm.	5-10	4-10	0.75
Medium pressure	5-9	5-8	0.75
Friedel and Anderson	1-20	3-20	0.85
<b>Iron Catalysts</b>			
Ruhrchemie	1-17	3-9	0.66
Rheinpreussen	1-17	3-10	0.67
Kaiser-Wilhelm-Institut	1-17	3-9	0.68
Lurgi	1-17	2-11	0.69
I.G. Farbenindustrie	1-17	1-9	0.66
Brabag	1-17	1-9	0.69
Standard Oil	1-16	3-11	0.66

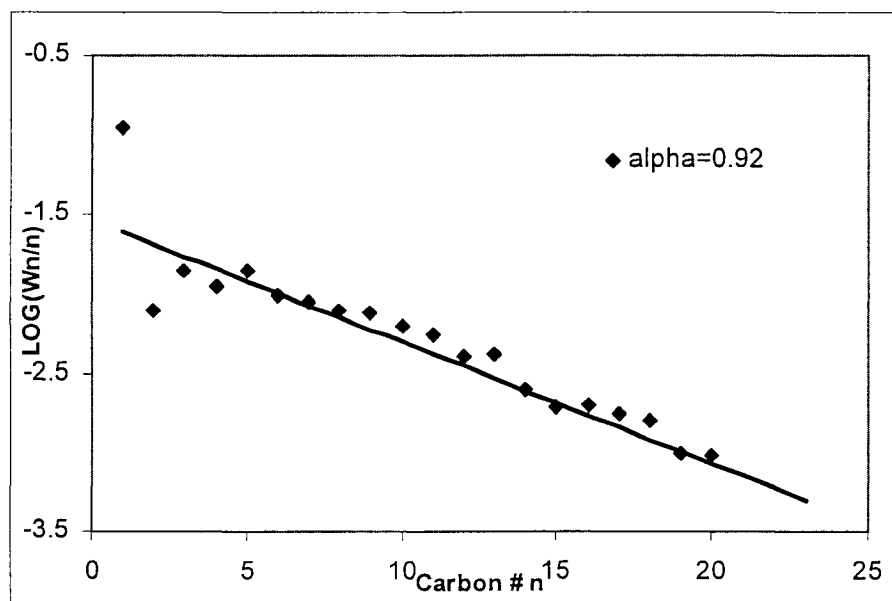


Figure 3. Product Distribution of F-T Synthesis Over Co Catalyst

Storch, Golumbic, and R.B. Anderson [11] (Study II) observed a linear correlation between  $\log(W_n/n)$  and carbon number  $n$  with a slope of  $\log \alpha$ , shown in Figure 3 of Fischer-Tropsch and related synthesis. This linear correlation is another characteristic expression of the Anderson-Shultz-Flory chain growth mechanism.

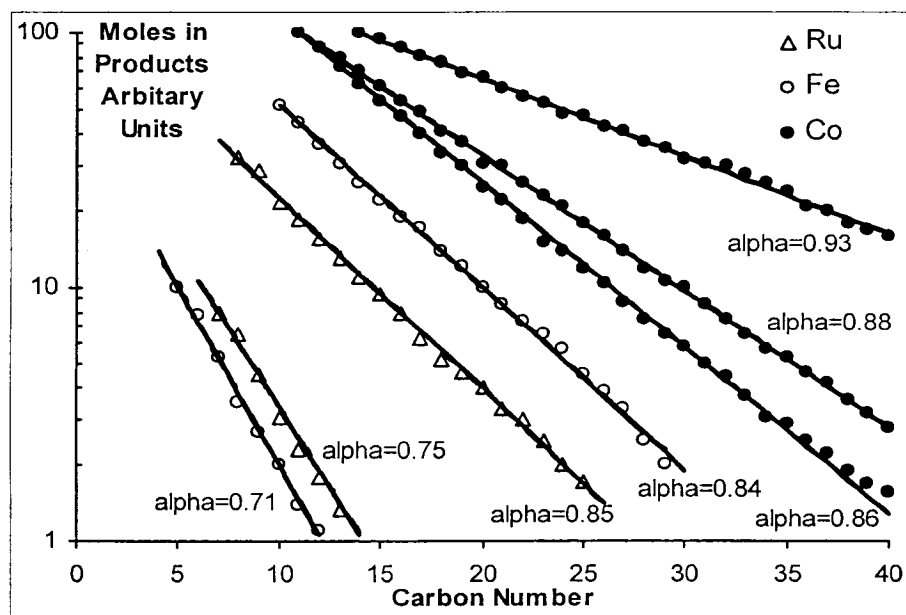


Figure 4. Typical Carbon Number Distribution of Co, Fe, and Ru Catalysts

Sie's [12,13] more recent investigation (Study III), in which a few hundred independent F-T synthesis experiments were carried out with various catalyst formulations under different operating conditions, found that the product distribution was indeed in close agreement with the Anderson-Shultz-Flory chain growth mechanism with a varying  $\alpha$  value, shown in Figure 4.

In Figures 3 and 4, the points are the experimental data reported in the classical F-T synthesis literature and the lines are the linear correlation of the ASF model developed by the reviewers of those data.

To examine the accuracy of the predictions of the user-defined model on F-T product selectivity, Study IV through Study XIII were analyzed. In this analysis, the values of the chain growth probability  $\alpha$ , used in the user-defined model to calculate the F-T product selectivity, were calculated by the correlations of F-T synthesis operating conditions parameters (type of catalysts, temperature, and pressure) described in the last part of this section.

For Figure 5 through Figure 10, experimental data reported in Study IV to Study X were compared to predicted results from the user-defined model on  $C_{5+}$  products selectivity to examine the accuracy of the simulation model's prediction of  $C_{5+}$



products selectivity. The values of  $\alpha$  to calculate the predicted product selectivity of each case were obtained by the correlations for the according type of catalysts described at the end of this section.

For Figures 5 through 7, the predicted results were compared to the experimental data on F-T  $C_{5+}$  product selectivity of Co catalysts. The values of  $\alpha$  to calculate the predicted product selectivity of each case were obtained by the second correlation for Co catalysts described later in this section.

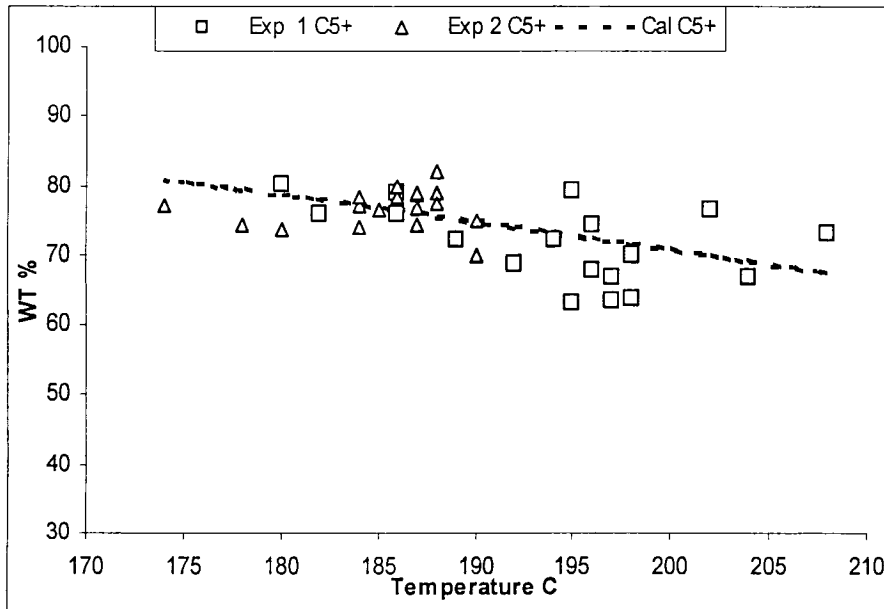


Figure 5. Experimental Data and Simulation Results of Co Catalysts -1

Figure 5 shows the comparison between the predicted and the experimental results of F-T synthesis  $C_{5+}$  products weight percent (WT %) under a pressure of 100 psi and a temperature range from 174°C to 208°C. Experimental data were adapted from Study IV of “Technical Paper 709” [14] from the Department of Energy. Different types of Co catalysts were used in the experiments. The model thus gives a general prediction of the  $C_{5+}$  products WT% of Co catalysts.

Figure 6 shows the comparison between the predicted and the experimental results of F-T Synthesis  $C_{5+}$  products selectivity of different Co catalysts types. Data of Experiment #1 are adapted from Study V of Chaumette [15] on the reactivity of Co catalysts at 220°C and 20 atm. Data of Experiment #2 are adapted from Study VI of Udaya [16] on bifunctional Co catalysts in syngas conversion at 280°C and 21atm.

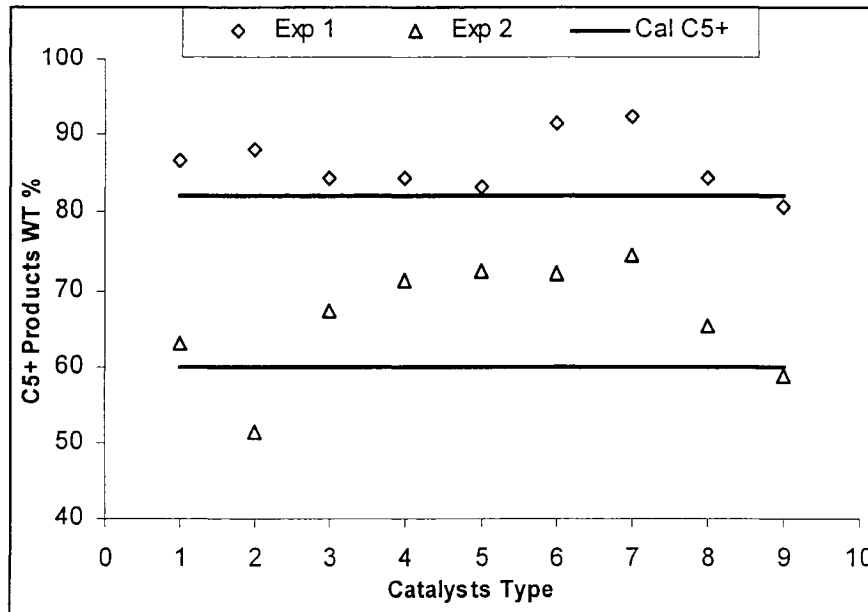


Figure 6. Experimental Data and Simulation Results of Co Catalysts -2

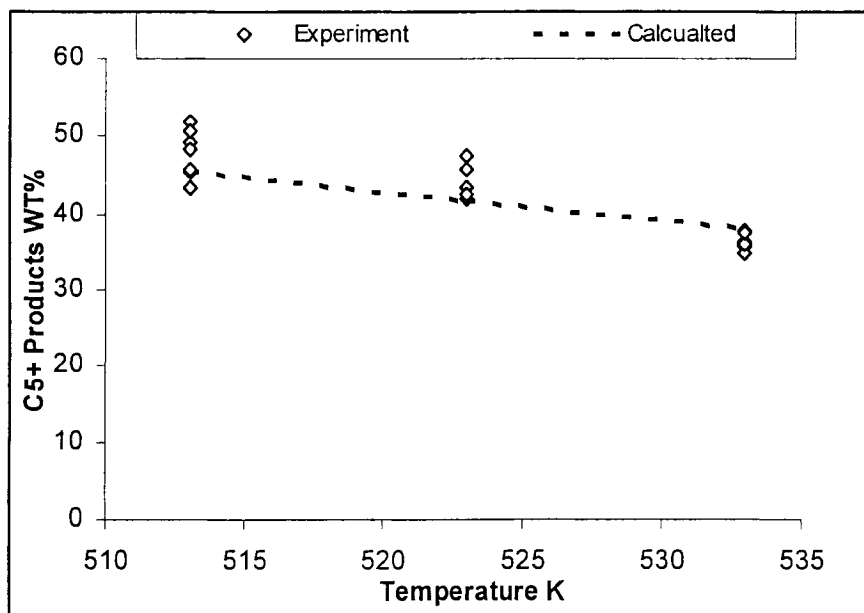


Figure 7. Experimental Data and Simulation Results of Co Catalysts -3

Sethuraman [19] conducted a series of experiments in Study X examining the production of  $C_4$  hydrocarbons from Fischer-Tropsch synthesis in a follow bed reactor using Co catalysts. The experiments, carried out at three temperature points: 513K, 523°K and 533°K at low reaction pressure, showed the temperature effect on F-T synthesis product selectivity.  $C_{5+}$  products WT% are plotted and compared with the simulation results in Figure 7. The model reasonably predicts

the temperature effect on the  $C_{5+}$  product WT% in the temperature range from 513°K to 533°K, as shown in Figure 7.

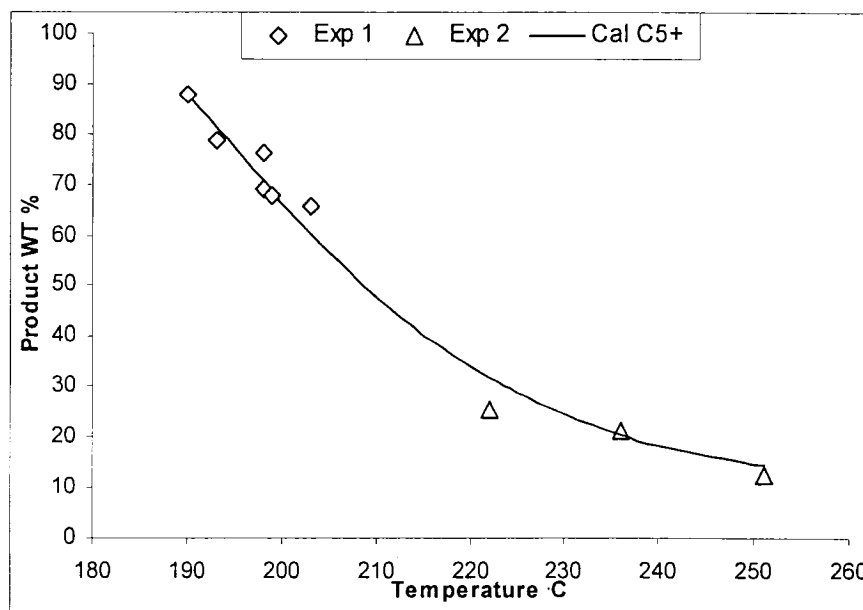


Figure 8. Experimental Data and Simulation Results of Ni Catalysts

Figure 8 shows the comparison between the predicted and the experimental results of Fischer-Tropsch Synthesis product distribution of Ni catalysts under the atmosphere pressure and in temperatures ranging from 190°C to 251°C. The values of  $\alpha$  used to calculate the predicted product selectivity of each case were obtained by the fourth correlation for Ni catalysts described later in this section. The data for Experiment #1 were adapted from Study IV, “Technical Paper 709” [14] from the Bureau of Mines. The data for Experiment #2 were adapted from Study VII, Hadjigeorghiou’s [17] work on F-T selectivity of Ni catalysts. Different types of Ni catalysts were used in the experiments. The model thus gives a general prediction of the  $C_{5+}$  products WT% of Ni catalysts.

Figure 9 shows the comparison between the predicted and the experimental results of Fischer-Tropsch synthesis product selectivity of Fe catalysts under a pressure of 7.8 atm and in temperatures ranging from 220°C to 260°C. The values of  $\alpha$  used to calculate the predicted product selectivity of each case were obtained by the first correlation for Fe catalysts described later in this section. Experimental data in Figure 8 were adapted from Study VIII, “Bulletin 578” [18] of the Bureau of Mines. Different types of Fe catalysts were used in the experiment. The model reasonably predicts the product selectivity (in groups of  $C_1$ ,  $C_3$ - $C_4$  and  $C_{5+}$ ) of Fe catalysts.

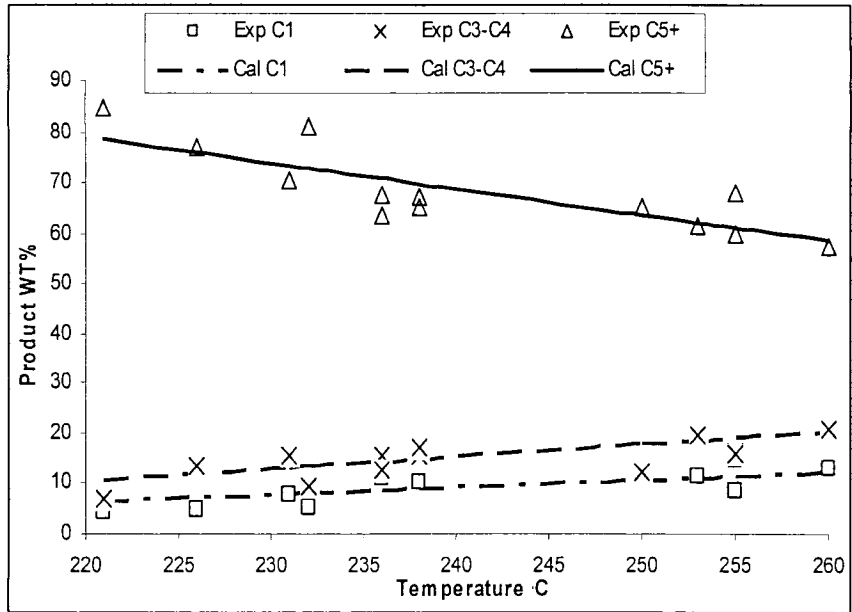


Figure 9. Experimental Data and Simulation Results of Fe Catalysts

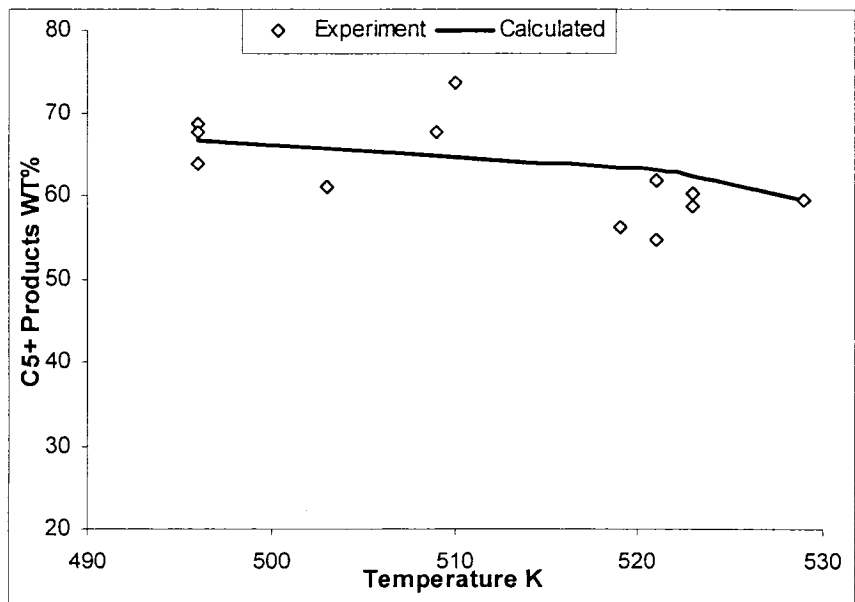


Figure 10. Experimental Data and Simulation Results of Ru Catalysts

Figure 10 shows the comparison between the predicted and the experimental results of Fischer-Tropsch synthesis product distributions of Ru catalysts under a medium pressure of about 8 bars and in temperatures ranging from 493°K to 529°K. The values of  $\alpha$  used to calculate the predicted product selectivity of each case were obtained by the third correlation for Ru catalysts described at the end of this

section. Experimental data in Figure 10 are adapted from Everson [20] on 0.5% Ruthenium-on-alumina catalyst (Study IX).

The simulation model gives a good prediction of the  $C_{5+}$  products selectivity of the four types of the four types of catalysts shown by the comparisons between the experimental data and predicted results in Figure 5 through Figure 10.

For Figures 11 and 16, the Fischer-Tropsch products yield data of commercial plants were compared with the predicted results from the user-defined model to examine the model's prediction accuracy on a more detailed F-T synthesis product selectivity. The values of  $\alpha$  used to calculate the predicted product selectivity of each case were obtained by the first correlation for Fe catalysts described later in this section. In Figure 11 through Figure 14 products were divided into four groups:  $C_1-C_4$  (fuel gas),  $C_5-C_{11}$  (naphtha),  $C_{12}-C_{18}$  (distillates), and  $C_{19+}$  (wax). In Figure 15 and Figure 16, they were divided into three groups:  $C_1-C_4$ ,  $C_5-C_{12}$ , and  $C_{13+}$ .

The SASOL Synthol plant operates at  $220^\circ\text{C}$  and 25atm using precipitated Fe catalysts in a fixed-bed reactor. The SASOL Arge plant operates at  $325^\circ\text{C}$  and 25atm using fused Fe catalysts in a circulating fluidized bed reactor. Figures 11 and 12 show the comparison between the data from SASOL reactors and the simulation results. The SASOL plant data were adapted from Rao's [21] technology review in Study XI on Fe-based catalysts for slurry-phase Fischer-Tropsch synthesis.

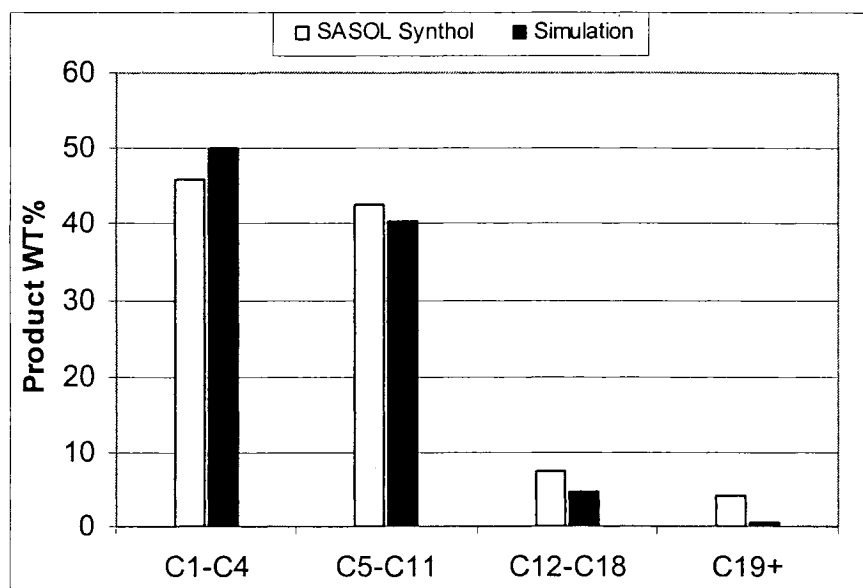


Figure 11. SASOL Synthol Plant Data and Simulation Results

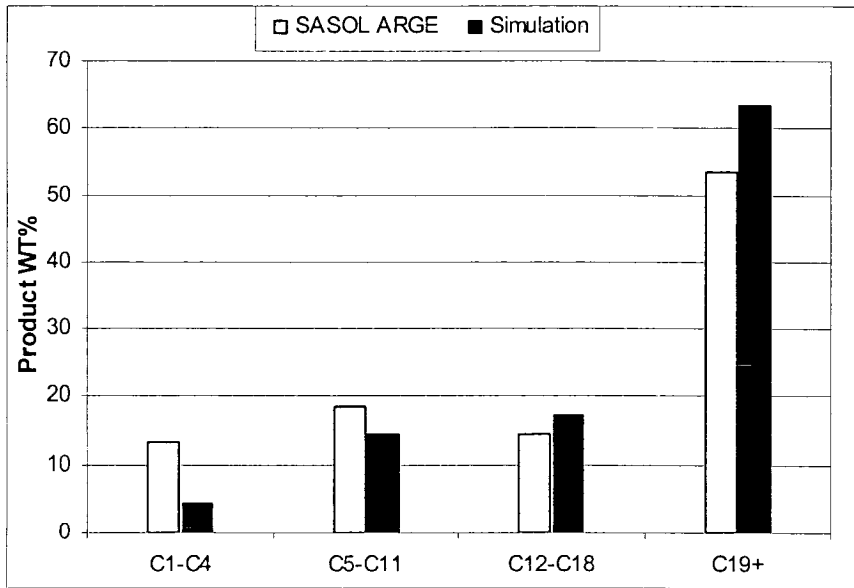


Figure 12. SASOL Arge Plant Data and Simulation Results

The Rheinprussen demonstration plant operates at 268°C and 12atm using 100Fe/0.1Cu/0.05-0.5K<sub>2</sub>O catalyst in a bubble-column slurry reactor. The plant data in Figure 13 were adapted from a study of Kobel [22], which were also reviewed by Rao [id.] in Study XI.

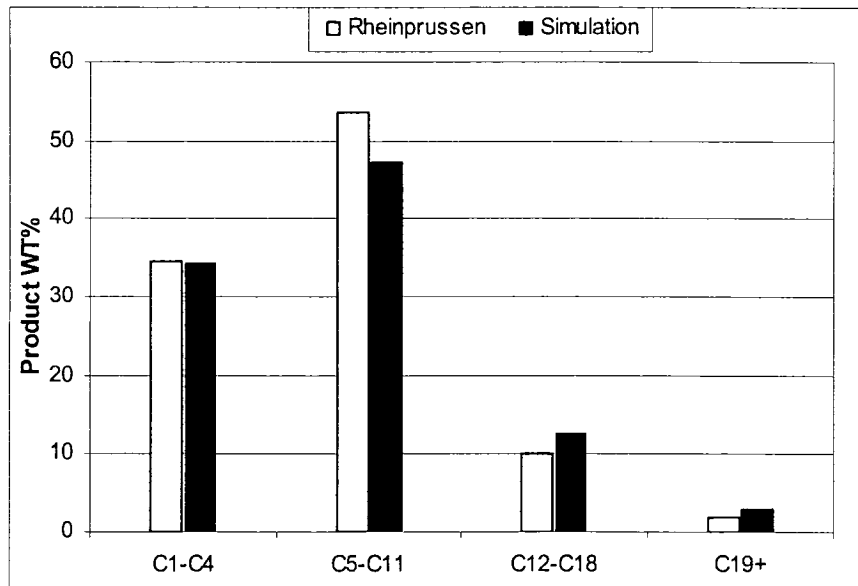


Figure 13. Rheinprussen Plant Data and Simulation Results

The Mobile plant operates at 260°C and 15atm using Fe/Cu/K<sub>2</sub>O catalyst in a bubble-column slurry reactor. The plant data in Figure 14 were adapted from Study XII of Kuo [23] on Mobile's two-stage process of converting syngas to transportation fuel.

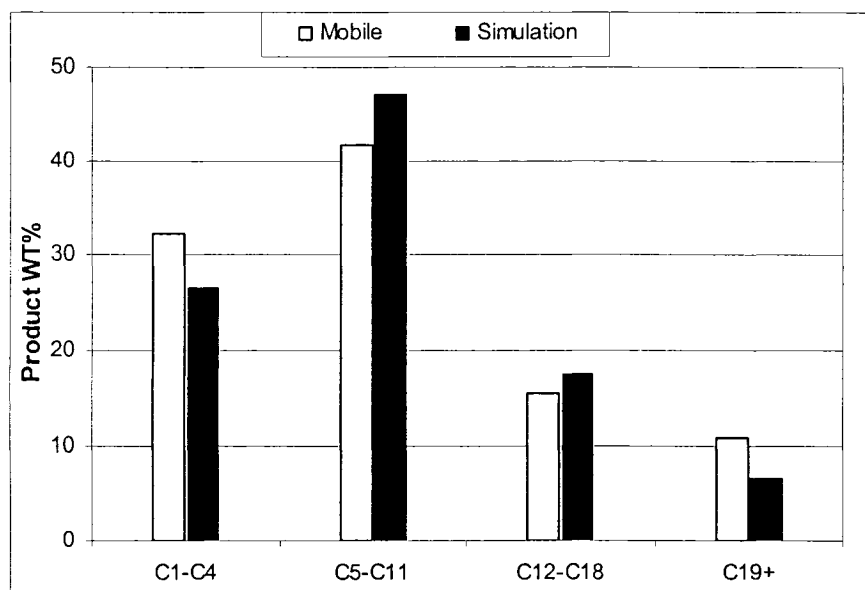


Figure 14. Mobile Plant Data Simulation Results

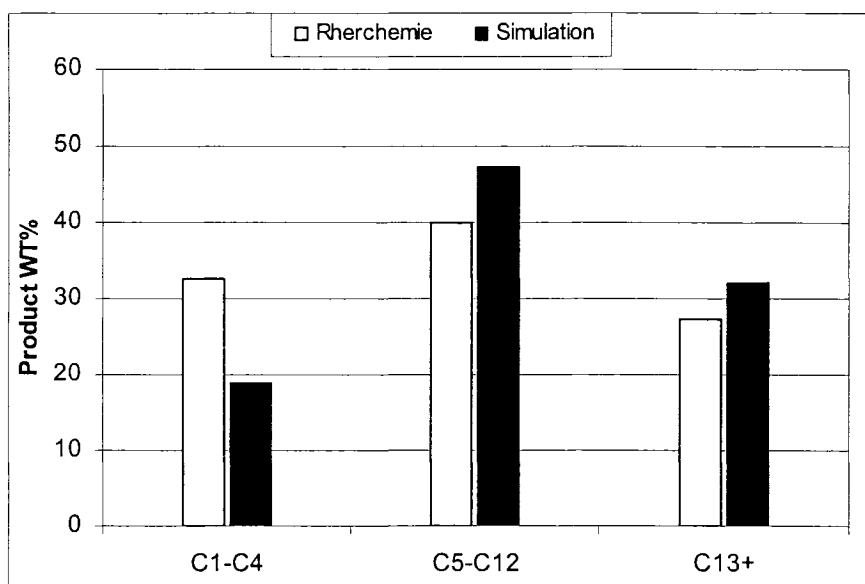


Figure 15. Satterfield's Data of Ruhrchemie Catalyst and Simulation Results

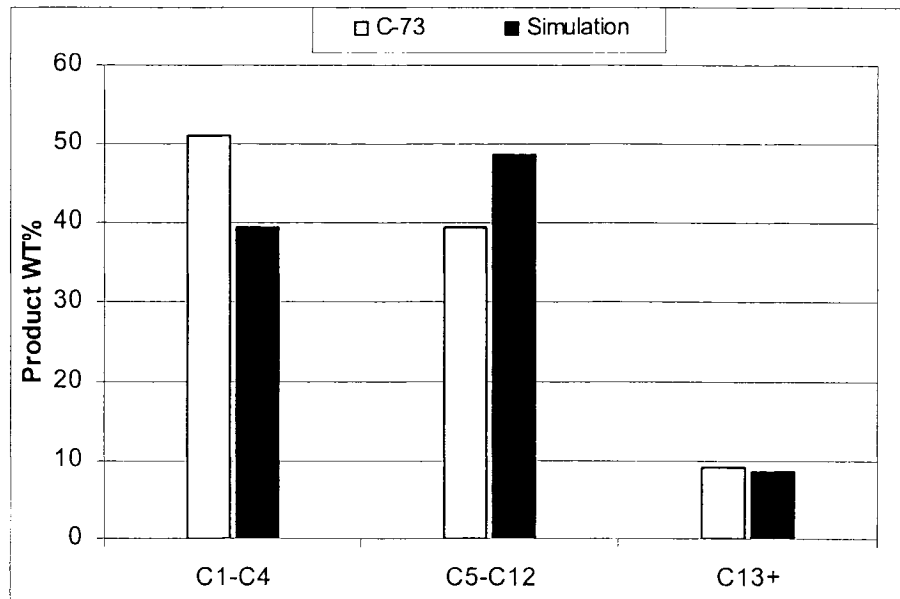


Figure 16. Satterfield's Data of C-73 Catalyst and Simulation Results

Satterfield and coworkers from MIT studied commercial catalysts' (Ruh Chemie and C-73 fused magnetic) activity and selectivity of Fischer-Tropsch synthesis. Ruh Chemie catalyst was tested at 263°C and 25atm. C-73 catalyst, an ammonia synthesis catalyst analogous to the fused magnetic catalyst used in the SASOL entrained bed F-T reactor, was tested at 263°C and 8atm. Both tests were done in a stirred tank slurry reactor. Srivastava [24] reviewed their data (Study XIII) and presented three products groups: C<sub>1</sub>-C<sub>4</sub> (fuel gas), C<sub>5</sub>-C<sub>12</sub> (naphtha), and C<sub>13+</sub> (distillates and wax). This was compared with the simulation results. Data in Figures 15 and 16 were adapted from Srivastava's review.

The user-defined model does reasonably predict the selectivity of the major F-T synthesis product groups as shown by the comparisons between commercial plant data and predicted results. The major groups are C<sub>1</sub>-C<sub>4</sub> (fuel gas), C<sub>5</sub>-C<sub>11</sub> (naphtha), C<sub>12</sub>-C<sub>18</sub> (distillates), and C<sub>19+</sub> (wax). In some cases, the major products groups are C<sub>1</sub>-C<sub>4</sub>, C<sub>5</sub>-C<sub>12</sub>, and C<sub>13+</sub>.

It is reasonable to use the user-defined model to predict the Fischer-Tropsch product selectivity in the ASPEN PLUS process flowsheet simulation as shown by comparing the predicted results and the reported experimental data.

The values of the chain growth probability,  $\alpha$ , used in the user-defined model to calculate the F-T product selectivity, were obtained from the correlations of F-T synthesis at various operating conditions and types of catalysts.



For each type of catalyst,  $\alpha$  is dependent on temperature and pressure. Following are the correlations developed for Fe, Co, Ru, and Ni catalysts.

1. Fe catalysts:  $\alpha = F_1(T, P)$

$$F_1(T, P) = A_1(T - T_0)^3 + B_1(T - T_0)^2 + C_1(T - T_0) + D_1 \ln P + E$$

$$A_1 = -4.57E-09, B_1 = 9.67E-06, C_1 = -2.39E-03, D_1 = 9.48E-02, E_1 = 2.98E-01;$$

2. Co catalysts:  $\alpha = F_2(T, P)$

$$F_2(T, P) = A_2(T - T_0)^3 + B_2(T - T_0)^2 + C_2(T - T_0) + D_2 \ln P + E_2$$

$$A_2 = 2.28E-08, B_2 = 2.26E-06, C_2 = -1.87E-03, D_2 = 8.75E-02, E_2 = 2.87E-01;$$

3. Ru catalysts:  $\alpha = F_3(T, P)$

$$F_3(T, P) = A_3(T - T_0)^3 + B_3(T - T_0)^2 + C_3(T - T_0) + D_3 \ln P + E_3$$

$$A_3 = -1.38E-06, B_3 = -6.65E-05, C_3 = -1.85E-03, D_3 = 1.23E-01, E_3 = 1.29E-01;$$

4. Ni catalysts:  $\alpha = F_4(T, P)$

$$F_4(T, P) = A_4(T - T_0)^3 + B_4(T - T_0)^2 + C_4(T - T_0) + D_4 \ln P + E_4$$

$$A_4 = -3.45E-07, B_4 = 4.55E-05, C_4 = -2.75E-03, D_4 = 6.23E-02, E_4 = 2.98E-01;$$

T is F-T reaction temperature in °K; P is F-T reaction pressure in psi; and  $T_0 = 523^\circ\text{K}$ .

Using these correlations in the user-defined model, the values of the chain growth probability of the F-T reaction were calculated and the user-defined model predicted the F-T product selectivity accounting for the effects of catalyst type, temperature, and pressure.

However, there were some errors between the predicted and experimental data. The predicted results were within 25% of the experimental results. The errors derive from the approximations applied in the user-defined model in the ASPEN PLUS process flowsheet simulation.

In some instances, the predicted results do not fit well to the experimental results of one kind of catalyst prepared by a certain method. This is because the correlation of the chain growth probability was based on the average value of the type of catalysts prepared by different methods in a certain range of temperature and pressure.

In some instances, if the F-T synthesis products only consist of olefins, the model is a perfect fit. However, such cases rarely happen. Paraffins and oxygenates are formed in most Fischer-Tropsch synthesis cases. Paraffins have almost the same

molecular weight as olefins, while the oxygenates' molecular weights will be significantly larger than olefins' with carbon numbers larger than 4. So the weight percentage of the F-T synthesis products with a certain carbon number range predicted by the model deviated from the experimental results significantly when a large amount of oxygenates formed in the F-T synthesis.

### III. INTRODUCTION AND DESCRIPTION OF ASPEN PLUS CAD SOFTWARE

ASPEN PLUS, developed by MIT in the late 1970's and commercialized by Aspen Tech in 1982, is a process modeling and simulation program. Because of its strict mechanistic model and advanced technique, ASPEN PLUS is used in many industries. It has broad applications in the chemical industry, including investigating alternative process flow sheets in research and development, optimizing plant and process schemes in design work, improving yield and throughput of existing plants, and training operators.

ASPEN PLUS simulates steady-state processes, also known as process flowsheeting. The basic unit of the flowsheet is the BLOCK model. Unit operations (reactors, distillation columns, etc.) and related operations can be plugged into BLOCK. The user can translate a process into an ASPEN PLUS simulation model by performing the following steps [6]:

1. Define the process flowsheet:
  - i. Define the unit operations in the process.
  - ii. Define the process streams that flow to and from the unit operations.
  - iii. Select BLOCK models from the ASPEN PLUS Model Library to describe each unit operation and place them on the process flowsheet.
  - iv. Place labeled streams on the process flowsheet and connect them to the unit operation models.
2. Specify the chemical components in the process. Components can be taken from ASPEN PLUS's built-in databanks or defined by the user.
3. Specify thermodynamic models to represent the physical properties of the components and mixtures in the process. These models are built into ASPEN PLUS.
4. Specify the component flow rates and the thermodynamic conditions (e.g., temperature, pressure, and composition) of the feed streams.
5. Specify the operating conditions for the unit operation models. Specifications, such as flowsheet configuration, operating conditions, and feed compositions, can be interactively changed to run new cases and analyze process alternatives.

ASPEN PLUS then solves the flowsheet sequentially for output streams given input streams properties and BLOCK parameters. In this way, the process flowsheet provides information about the process for the model, such as, configuration of unit operations along with operating conditions, feed stream compositions, and flow rates. The simulation also predicts the performance of the plant by computing the flow and properties of all intermediate and product streams, the performance of every unit in the process, and the capital and operating costs of the plant. With ASPEN PLUS, the user can interactively change specifications, such as flowsheet configuration, operating conditions, and feed compositions, to run new cases and analyze process alternatives. In addition to the process simulation, ASPEN PLUS allows the user to perform a wide range of other tasks such as estimating and regressing physical properties, generating custom graphical and tabular output results, fitting plant data to simulation models, optimizing the process, and interfacing results to spreadsheets.

Aspen Tech recently announced ASPEN PLUS Release 11.1. The new version incorporates new engineering features in all key areas, including equipment design and rating calculations, petroleum modeling, distillation and separations, physical properties, reactor and other unit operation models, and cost and economic evaluation, among others. This version also includes a new capability, Data-Fit, to help fit simulation models to plant or laboratory data, thus providing a path from raw plant data to a simulator model that matches actual operation.

Computer Aided Design (CAD) was utilized to evaluate the conversion processes of coal to liquid fuels by Fischer-Tropsch synthesis. Simulations based on the mechanisms of the F-T process and other processes involved were run in ASPEN PLUS 11.1. Process flow sheet (PFS) simulations consisted of two parts: Syngas Generation & Cleanup and Fischer-Tropsch Synthesis. A reactor model minimizing the Gibbs free energy simulated the coal gasification process (Shell Coal Gasification). A user-defined model simulated the Fischer-Tropsch synthesis, calculating the F-T synthesis product distribution by applying the Anderson-Schulz-Flory distribution model to this user-defined model. Several cases with different operating conditions of Fischer-Tropsch synthesis were specified to examine their effects.

This CAD simulation is described in the following chapter.

#### IV. PROCESS FLOWSHEET MODEL DESCRIPTION

In this chapter, the ASPEN PLUS process flowsheet simulation model of the Fischer-Tropsch conversion of coal to liquid fuels is described.

Conversion of coal to liquid fuels by F-T Synthesis is an indirect coal liquefaction process. The coal is first ground to a particle size of less than  $100\mu\text{m}$  ( $10^{-4}\text{m}$ ) diameter, then dried to the target water content required by the Shell Coal Gasification process. The dried coal is converted into syngas (mainly CO and  $\text{H}_2$ ) in a coal gasification reactor with an oxygen stream to produce a syngas mixture, which is then used as a feedstock to produce higher molecular weight hydrocarbons by F-T synthesis. After further processing involving cooling and cleaning, the syngas is sent to a CO shift reactor in which the  $\text{H}_2/\text{CO}$  ratio is raised to about 2.0. If an iron-based catalyst is used in F-T synthesis, this step is not required because the capacity of the iron-based catalyst for hydrogen production via the water-gas shift reaction. In a subsequent step in F-T synthesis, a metallic catalyst will produce hydrocarbons of higher molecular weight at elevated temperature and pressure. After product recovery and further treatment, gasoline, diesel fuel, and other liquid fuels are obtained. These steps will be described in more detail in the following sections.

The first part of the simulation model is the syngas generation and preparation area, including the Coal Drying, Coal Gasification, and Syngas Cooling & Cleanup Plants. The second section is the Fischer-Tropsch synthesis and product recovery area, including the CO Shift, Fischer-Tropsch Synthesis, and Product Recovery Plants. Individual plant model components will be described in the following sections.

The Coal Gasification (syngas generation process), CO Shift (water-gas shift process), and Fischer-Tropsch Synthesis Plants are the three major plant models where the chemical reactions are taking place in the ASPEN PLUS flowsheet simulation.

The Coal Gasification plant was based on the Shell Gasification process minimizing the Gibbs free energy for the syngas generation with the feed of dried coal and oxygen. This model, in mass and elemental balance, is designed to predict the connect flow rate of the syngas and ash production and the composition of the syngas produced.

The CO Shift Plant uses the thermodynamic equilibrium model to represent hydrogen production in a water-gas shift reactor. This model, in mass and elemental balance, is designed to set the  $\text{H}_2/\text{CO}$  ratio in syngas to the stoichiometric value of about 2.0 for the F-T synthesis. .

The Fischer-Tropsch Synthesis Plant uses a user-defined empirical model incorporating a Microsoft Excel spreadsheet to simulate the chain growth kinetics (Anderson-Shultz-Flory equation) of the Fischer-Tropsch synthesis. This model is elementally balanced.

### A. Individual Plant Components of Section 1: Syngas Generation and Preparation

This section describes the simulations of the Coal Drying Process, Shell Gasification Process, and Syngas Cooling & Cleanup Process. This processing area receives the wet ground coal particles, which are smaller than 100 $\mu$ m, and dries and gasifies them to produce syngas. This is the only processing area of the whole simulation model where solids are present. So ASPEN PLUS stream class MIXNCPD that contains substreams MIXED (to handle conventional components that reach vapor-liquid-solid phase equilibrium), CIPSD (to handle conventional components that appear in the solid phase but do not participate in phase equilibrium), and NCPD (to handle nonconventional components) was specified.

#### 1. Plant 101 Coal Drying Plant

The ground wet coal from Wyoming's Powder River Basin containing about 35% moisture was dried to 2% moisture by a hot nitrogen stream at 450°F under atmosphere pressure in a multi-stage stacked fluidized coal drying unit (Plant 101).

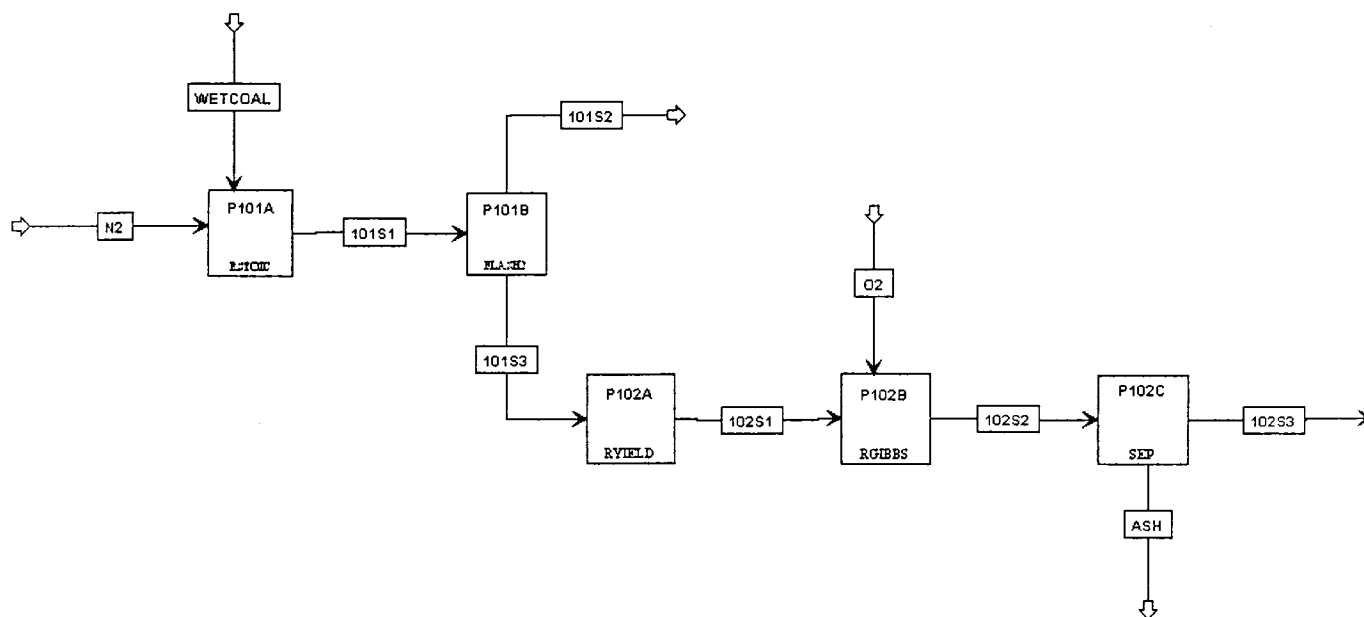


Figure 17. ASPEN PLUS Flowsheet of Plant 101 and Plant 102

Two ASPEN PLUS unit operation blocks simulated Plant 101: RESTOIC (P101A) and FLASH2 (P101B). Both blocks are isobaric and adiabatic. P101A modeled the drying of coal from 35% moisture to 2%. P101A produced a single outlet stream (101S1). P101B modeled the separation of the dried coal particles stream (101S3) from the moist nitrogen stream (101S2). The physical property parameters of the coal and nitrogen of the feeds are shown in Table 4 and Table 5.

Table 4. Properties of the Feeds to Plant 201

Feed	WET COAL	N2
Substream	NCPSD	MIXED
Temperature F	77	450
Pressure psi	14.7	14.7
Mass Vapor Frac	0	1
Mass Solid Frac	1	0
Mass Flow lb/hr	2537034	7500000

Table 5. Physical Properties of Raw Coal

Elements	WT%
ASH	5.9
CARBON	75.6
HYDROGEN	6
NITROGEN	0.7
CHLORINE	0
SULFUR	0.9
OXYGEN	16.8
<b>Other Component</b>	
MOISTURE WT % in feed	35
ASH	5.9
MOISTURE WT% after drying	2
Lower heating value Btu/lb	7380

## 2. Plant 102 Shell Gasification Plant

The Shell Coal Gasification process (SCG process) took place in Plant 102. The SCG process for the gasification of coal under pressure is based on the principles of entrained-bed technology. The feeds were the dried coal from Plant 101 and oxygen from air separation plant. The reactor was basically an empty vessel, providing a residence time of a few seconds under a pressure of 430 psi. The reactor temperature was as much as 3700°F (2000°C), but the reactor outlet temperature was normally about 2800°F (1500°C). Under these operating



conditions the coal was virtually completely gasified without the formation of tars, phenols, or the condensate hydrocarbons. The overall carbon conversion was about 99 percent. [8]

Three ASPEN PLUS unit operation blocks simulated Plant 102: a RYIELD (P102A), a RGIBBS (P102B), and a SEP (P103C). The RGIBBS model (P102B) simulated Shell Gasification of the coal by minimizing the Gibbs free energy with the feed of the dried coal and oxygen. However, the Gibbs free energy of the coal could not be calculated because the coal is a nonconventional component. Before feeding the dried coal (101S3) to RGIBBS block, RYIELD block (P102A) decomposed the coal into its constituent components. Finally the SEP (P102C) modeled the separation of the product raw gases (102S2) from the residual ash (ASH). The residual ash was removed by a combination of mechanical processes, usually cyclones, electrostatic methods, and water washing processes.

### 3. Plant 103 Syngas Cooling & Cleanup Plant

In Plant 103, two syngas coolers cooled the syngas from Plant 102 to about 1000°F and reduced the pressure to 130 psi. A water quench tower removed the impurities such as H<sub>2</sub>S, CO<sub>2</sub>, SO<sub>x</sub>, and NO<sub>x</sub> from the cooled syngas stream (103S3) and cooled the syngas to 100°F at 130 psi.

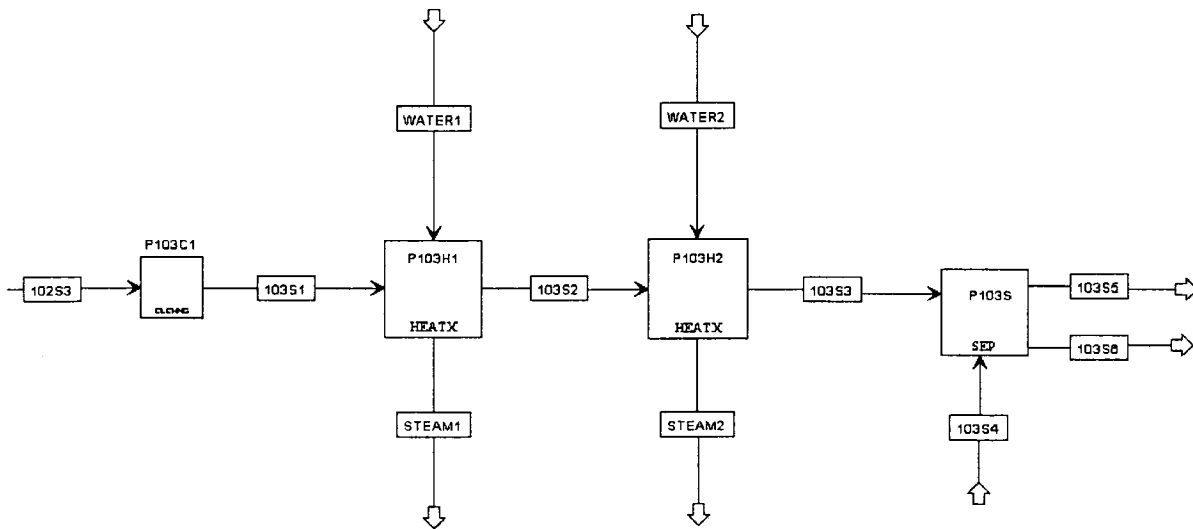


Figure 18. ASPEN PLUS Flowsheet of Plant 103

Because there is no solid contained in the syngas stream (102S3), an ASPEN PLUS class changer block (P103C1) changed the stream class from MCINCPD to CONVEN, which only contains MIXED substream. This change of the stream class simplified the subsequent ASPEN PLUS process block models and sped up the simulation. Two HEATX unit operation blocks, P103H1 and P103H2, then



simulated the syngas cooling process. Two water streams were added into these two blocks and two steams, 975 psi / 750°F and 530 psi / 530°F, were generated. These two high pressure steams were used in other plants. A simple ASPEN PLUS component separator block SEP (P103S) simulated the syngas cleanup processes. Stream 103S5 was the clean moist syngas stream and stream 103S6 was the wastewater stream.

## B. Individual Plant Components of Section 2: Fischer-Tropsch Synthesis and Product Recovery

This section describes the CO Shift process (Plant 201), Fischer-Tropsch Synthesis process (Plant 202), and Product Recovery Process (Plant 203). This area processed clean syngas from Plant 103 using the water-gas shift reaction to raise the H<sub>2</sub>/CO ratio to the stoichiometric value of about 2.0 for the Fischer-Tropsch Synthesis plant, which produced fuel gas, liquid fuels, and wax. The hydrocarbon recovery plant collected the liquid products from the previous plant and separated them into product streams for further processing. Because there was no solid present in this processing area, all the streams in this part of the model were classified as the ASPEN PLUS stream class CONVEN, which has only one substream MIXED that contains only conventional component.

### 1. Plant 201 CO Shift Plant

The clean syngas stream from Plant 103 must go through a CO Shift Plant to raise the H<sub>2</sub>/CO ratio to the stoichiometric value of about 2.0 for the Fischer-Tropsch synthesis. (If some iron-based catalysts are used in F-T synthesis, this plant is not necessary due to the water-gas shift activity that makes hydrogen from the iron-based catalysts.) The syngas was heated to 675°F before entering a high temperature shift converter where the CO reacted with water to produce H<sub>2</sub> and CO<sub>2</sub>. The exiting gas was cooled and the CO<sub>2</sub> removed.

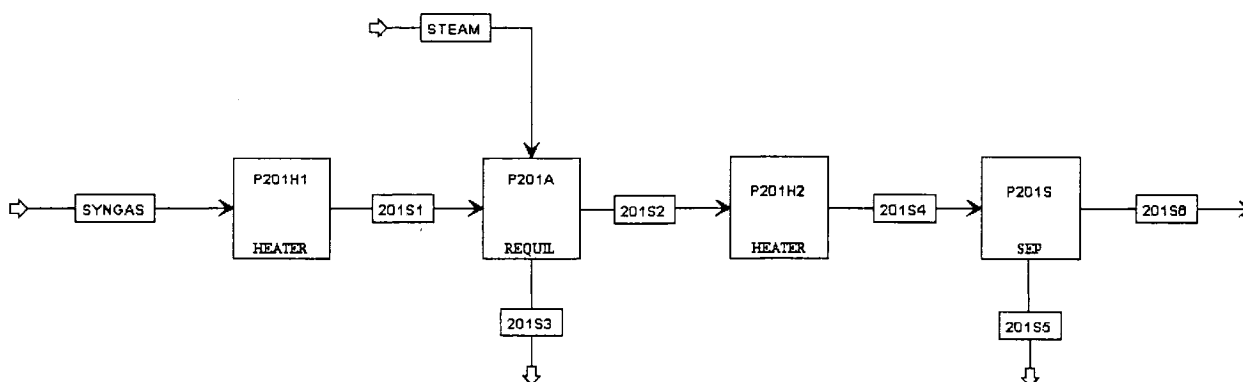


Figure 19. ASPEN PLUS Flowsheet of Plant 201

Four ASPEN PLUS unit operation blocks simulated Plant 201. The syngas was heated to 675°F in a HEATER block (P201H1) and then mixed with the 430°F / 360 psi steam. An ASPEN REQUIL block (P201A) simulated a high temperature equilibrium shift converter where the CO reacted with water to produce H<sub>2</sub> and CO<sub>2</sub>. A 50°F approach (difference) to equilibrium is specified in this model. Stream 202S3 was a null liquid stream required by the REQUIL block. The exiting gas stream (201S2) was then cooled by a HEATER block (P201H2) and a FLASH2 block (P201S). P202H2 represented a series of air coolers that cooled the effluent to 300°F. Block P202S represented a gas wash tower, which simultaneously cooled the gas to 200°F and separated 99% of the CO<sub>2</sub> produced in the CO shift reaction from the syngas with fresh cooling water.

## 2. Plant 202 Fischer-Tropsch Synthesis Plant

After compression to about 360 psi in a multistage compressor, the shifted syngas from Plant 201 was converted into hydrocarbon products in a tubular reactor, which is similar to a shell and tube heat exchanger, by Fischer-Tropsch synthesis. The tubes were filled with catalyst and hot reactant gases flow through them. The hydrocarbon products from F-T synthesis varied from C<sub>1</sub> to about C<sub>60</sub>, from paraffins to olefins and oxygenates. The F-T reactor generated a vapor stream, which contained light hydrocarbons, and a liquid stream that contained wax products. These two streams were then sent to the hydrocarbon recovery plant for further treatment.

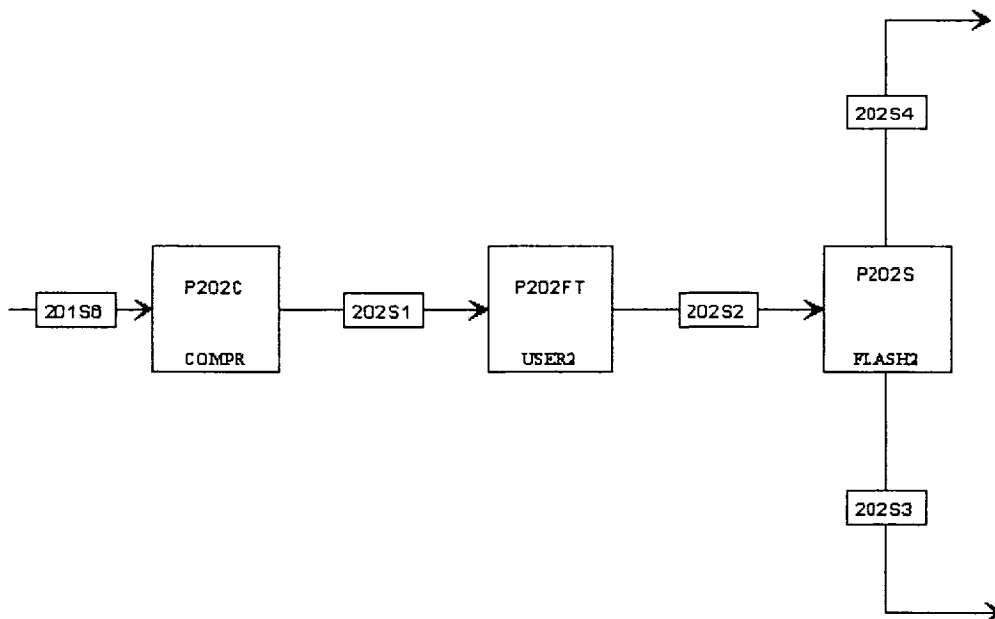


Figure 20. ASPEN PLUS Flowsheet of Plant 202

Three ASPEN PLUS blocks simulated Plant 202. A COMPR block simulated the syngas compressor, which compressed the syngas from the CO shift plant to 350 psi. A user-defined model (P201FT) simulated the F-T reaction and predicted the F-T synthesis yields. Block P202FT also flashed its outlet stream (202S2) to 500°F and 350 psi, which represented the temperature and pressure of the reactor outlet effluent. A FLASH2 block represented the primary wax separator, which performed an equilibrium calculation on the total reactor effluent to generate vapor and liquid streams. The liquid stream (202S3) that contained mostly wax and the vapor stream (202S4) that contained lighter products were sent to the hydrocarbon recovery plant for further treatment.

To represent the C<sub>1</sub>-C<sub>20</sub> hydrocarbons produced in Fischer-Tropsch synthesis, paraffins and  $\alpha$ -olefins with carbon numbers ranging from 1 to 20 were chosen from the ASPEN PLUS databank. The user defined an additional ten pseudo-components of C<sub>21</sub>OP through C<sub>29</sub>OP (representing a mixture of wax in the C<sub>21</sub> through C<sub>29</sub> carbon range) and C<sub>30</sub>WAX (representing a mixture of C<sub>30+</sub> wax) in the ASPEN PLUS component list to characterize the raw C<sub>21+</sub> Fischer-Tropsch wax. Three pseudo-components, OXVAP, OXHC, and OXH<sub>2</sub>O, were also defined to represent oxygenates produced in F-T synthesis. The basic properties (gravity, molecular weight, and boiling point) of pseudo-components C<sub>21</sub>OP through C<sub>29</sub>OP, C<sub>30</sub>WAX, OXVAP, OXHC, and OXH<sub>2</sub>O were supplied before the simulation model was executed.

The user-defined model block (P202FT) was an empirical model that contains the F-T synthesis yields correlations, developed from the Anderson-Schulz-Flory equation described in Chapter II, and was elementally balanced. It required three user input parameters: the reactor temperature, the reactor pressure, and the type of catalyst used in the F-T reaction. A Microsoft Excel spreadsheet was incorporated into this user-defined model to calculate each mass flow rate of hydrocarbon produced in F-T synthesis with two variables, the chain growth probability and the CO conversion percentage, which were both dependent on the user input parameters of block P202FT.

This user-defined model block (P202FT) used two REAL input parameters and four INTEGER input parameters. The two user REAL parameters were F-T reactor temperature (T) and pressure (P). The values of these two parameters were used in the Microsoft Excel spreadsheet to calculate the values of the chain growth probability- $\alpha$  of each catalyst type and CO conversion percentage, both were then used to calculate the mass flows of the F-T products. An Interface program between ASPEN PLUS and MS Excel Spreadsheet collected the values of the products' mass flows and then those values were loaded into the output stream (202S2) of block P202FT.

The values of chain growth probability of the four types of catalysts were calculated using the four correlations described in Chapter II:

1. Fe catalysts:  $\alpha = F_1(T, P)$

$$F_1(T, P) = A_1(T - T_0)^3 + B_1(T - T_0)^2 + C_1(T - T_0) + D_1 \ln P + E$$

$$A_1 = -4.57E-09, B_1 = 9.67E-06, C_1 = -2.39E-03, D_1 = 9.48E-02, E_1 = 2.98E-01;$$

2. Co catalysts:  $\alpha = F_2(T, P)$

$$F_2(T, P) = A_2(T - T_0)^3 + B_2(T - T_0)^2 + C_2(T - T_0) + D_2 \ln P + E_2$$

$$A_2 = 2.28E-08, B_2 = 2.26E-06, C_2 = -1.87E-03, D_2 = 8.75E-02, E_2 = 2.87E-01;$$

3. Ru catalysts:  $\alpha = F_3(T, P)$

$$F_3(T, P) = A_3(T - T_0)^3 + B_3(T - T_0)^2 + C_3(T - T_0) + D_3 \ln P + E_3$$

$$A_3 = -1.38E-06, B_3 = -6.65E-05, C_3 = -1.85E-03, D_3 = 1.23E-01, E_3 = 1.29E-01;$$

4. Ni catalysts:  $\alpha = F_4(T, P)$

$$F_4(T, P) = A_4(T - T_0)^3 + B_4(T - T_0)^2 + C_4(T - T_0) + D_4 \ln P + E_4$$

$$A_4 = -3.45E-07, B_4 = 4.55E-05, C_4 = -2.75E-03, D_4 = 6.23E-02, E_4 = 2.98E-01;$$

T is F-T reaction temperature in °K; P is F-T reaction pressure in Psi;  $T_0 = 523$  °K.

The four INTEGER parameters were used to specify the type of the catalysts and had a value of either 1 or 0. (Only one “1” should be specified in all of the four INTEGER parameters.) The types of the catalysts were arranged in the order of Fe, Co, Ru, and Ni. If “1 0 0 0” was specified, Fe catalyst was used; if “0 0 1 0” is specified, Ru catalyst was used. In this way, the value of chain growth probability was calculated by the equation

$$\alpha = A \times F_1(T, P) + B \times F_2(T, P) + C \times F_3(T, P) + D \times F_4(T, P)$$

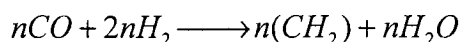
A, B, C, and D are the values of the four input INTEGER parameters.

Specifying the CO conversion percentage,  $X_{CO}$ , was equivalent to specifying the  $H_2$  conversion percentage because the two are related by the stoichiometry of the F-T Synthesis.  $X_{CO}$  was calculated using the correlation of F-T reaction temperature and pressure below:

$$X_{CO} = 13.5 \ln(P/15)/100 + 0.252 e^{T/3000}$$

P is F-T reaction pressure in Psi and T is temperature in °K.

As long as the CO conversion percentage was calculated, the total amount of the hydrocarbon produced in F-T synthesis  $W$  could be calculated with the input of mole flow rates of CO and H<sub>2</sub> according the stoichiometric equation below.



Mass fractions  $W_n$  of the F-T products except oxygenates were calculated using the ASF equation below. The carbon number  $n$  was as large as 100.

$$\log(W_n / n) = n \log \alpha + \log[(1 - \alpha)^2 / \alpha]$$

It is often observed that the selectivity of the F-T products with carbon number  $n$  smaller than 4 does not obey the Anderson-Shultz-Flory distribution model. For example, a low mass fraction value of C<sub>2</sub> is quite characteristic. Adjustments were made for the mass fractions of the C<sub>1</sub> to C<sub>4</sub> products as well as the mass fractions of oxygenate in order to produce a reasonable prediction on the selectivity of these F-T products.

$$W_1 = K \times W_0$$

$$W_2 = L \times W_0$$

$$W_3 = M \times W_0$$

$$W_4 = N \times W_0$$

$$W_{OXVAP} = P \times W_{oxygenates}$$

$$W_{OXHC} = Q \times W_{oxygenates}$$

$$W_{OXH@O} = R \times W_{oxygenates}$$

$$W_0 = 1 - W_{oxygenates} - \sum_{i=4}^{100} W_i ; W_{oxygenates} = \theta (1 - \sum_{i=4}^{100} W_i).$$

$K=0.55, L=0.10, M=0.2, N=0.2; P=1/12, Q=1/3, R=1/4; \theta=0.08;$

Thus, all of mass flow rates of the F-T products can be obtained by

$$M_n = W_n \times W \quad n = 1, 2, 3, \dots, 100;$$

and

$$M_{oxygenates} = W_{oxygenates} \times W$$

An Interface program between ASPEN PLUS and MS Excel spreadsheet collected the values of the mass flow rates of the F-T products and these values were loaded into the output stream (202S2) of block P202FT.

### 3. Plant 203 Hydrocarbon Products Recovery Plant

Plant 203 recovered the products from the F-T Synthesis, C<sub>4</sub> and lighter materials, C<sub>5+</sub> naphtha, distillates, and wax, for further processing. In this plant, several coolers cooled the two streams from Plant 202 to specified temperatures and a series of fractionation towers generated a low pressure fuel gas stream, a waste water stream, and three streams for further processing: a light C<sub>5+</sub> naphtha stream, a distillate stream, and a wax stream.

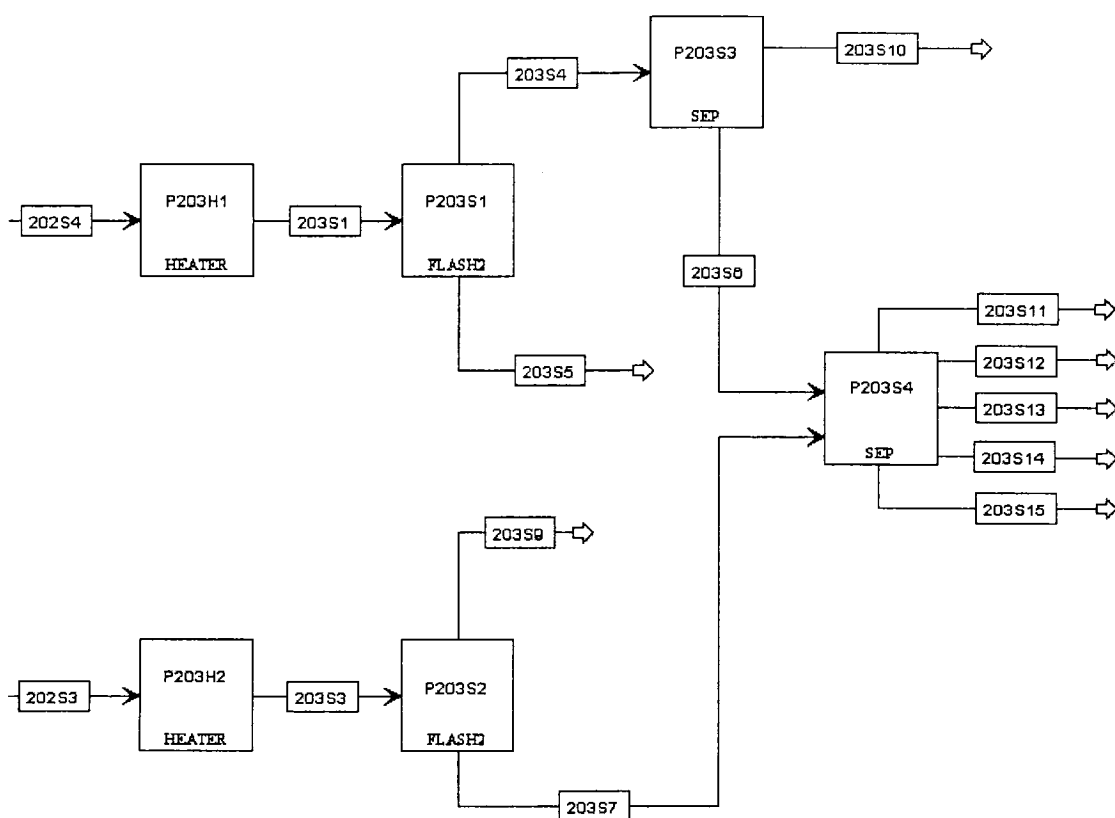


Figure 21. ASPEN PLUS Flowsheet of Plant 203

Two HEATER blocks, two SEP blocks and two FLASH2 blocks simulated Plant 203. The liquid reactor stream (202S3) was cooled to 200°F in a heat exchanger block (P203H2) and then flashed in a flash block (P203S2). The overhead stream of the flash became low pressure fuel gas while the bottom wax stream received further treatment in a series of fractionation towers (P203S4). The hot vapor overhead stream (202S4) from Plant 202 was cooled to 150°F in a heat exchanger

block (P203H1) and then sent to two separator blocks (P203S1 and P203S3). These two blocks generated a waste water stream (203S5), a liquid hydrocarbon stream (203S5), and a vapor stream (203S10). The liquid stream was further separated at P203S4 and the unconverted syngas together with  $C_1-C_4$  hydrocarbons became to high pressure fuel gas. A separator block (P203S4) collected the two liquid streams from the previous flash blocks (P203S2 and P203S3) and separated them into five streams: a low pressure fuel gas (203S11), a  $C_{5+}$  naphtha stream (203S12), a distillate stream (203S13), a wax stream (203S14), and a waste water stream (203S15).

The three product streams, light  $C_{5+}$  naphtha, distillate, and wax, were sent to regular petroleum refinery units to produce upgraded products. The wax stream will be catalytically hydrocracked to yield more desirable naphtha and distillate products. The naphtha and distillate streams together with the streams produced in the wax hydrocracking unit will be hydrotreated to produce high quality gasoline and diesel blending stocks. [9] However, the development of a process design for such refinery and hydrotreating units is beyond the scope of this paper.

## V. RESULTS OF PROCESS FLOWSHEET SIMULATION

This chapter describes the results of the process flowsheet simulations. A base case was selected and several other cases were simulated to predict the effects of varying Fischer-Tropsch synthesis operating conditions, catalyst type, temperature, and pressure on final product selectivity.

In the following sections, the base case operating conditions were 3000°K and 430 psi of the coal gasification process; a 283°K approach to equilibrium in the water-gas shift reactor and 525°K and 450 psi, with Co catalysts in the Fischer-Tropsch synthesis. For the other cases, only the parameter configuration (catalyst type, temperature, and pressure) of the F-T synthesis process (block P202FT) was changed, while the parameter configurations of the other plants remained the same.

### A. Case I – Base Case

The input of the base case simulation was a coal stream containing 35% moisture. This coal stream is configured with the same component fractions as Wyoming Powder River Basin coal. Through drying, gasification to syngas, and Fischer-Tropsch synthesis, the coal was converted into fuel gas, gasoline, diesel fuel, and wax. The details of the parameter specifications of the individual plants for the base case are described in detail in Chapter IV. Following are the results of the process flowsheet simulation.

The mole composition of the syngas stream (102S3) from the Coal Gasification Plant (Plant 102) obtained from the ASPEN PLUS flowsheet simulation is almost the same as the typical raw gas mole composition after solid removal of the Shell Gasification Process in Table 6 [8]. Table 7 shows the output streams composition of Plant 102.

Table 6. Typical Gas Composition After Shell Gasification Process

Constituent	Mol %
H <sub>2</sub> O	2
H <sub>2</sub>	28.5
CO	65.5
CO <sub>2</sub>	1.5
CH <sub>4</sub>	0.1
H <sub>2</sub> S	1.4
N <sub>2</sub> , Ar	1



Table 7. Output of Plant 102 (Stream 102S3 and Stream ASH)

Stream Name	102S3	ASH
Substream	MIXED	NCPSD
Temperature °F	2732	3632
Pressure psi	430	430
Mass Flow lb/hr	3.744E+6	1.147E+5
<b>Component</b>	<b>Mole %</b>	
H <sub>2</sub> O	3.914	0
N <sub>2</sub>	0.298	0
NO <sub>2</sub>	Trace	0
NO	Trace	0
SO <sub>2</sub>	2.13E-04	0
SO <sub>3</sub>	Trace	0
H <sub>2</sub>	28.614	0
CO	65.240	0
CO <sub>2</sub>	1.634	0
H <sub>2</sub> S	0.298	0
CH <sub>4</sub>	3.37E-04	0
ASH	0	100

Table 8 shows the simulation results of stream 103S5, the output of the Syngas Cooling & Cleanup Plant (Plant 103). Table 9 shows the simulation results of the CO Shift Plant (Plant 201).

Table 8. Output of Plant 103 (Stream 103S5)

	103S5
Temperature F	100
Pressure psi	130
Vapor Frac	1
Mole Flow lbmol/hr	1.837E+5
Mass Flow lb/hr	3.670E+6
<b>Component</b>	<b>Mole Frac</b>
H <sub>2</sub> O	0.06201
N <sub>2</sub>	0.00296
H <sub>2</sub>	0.28507
CO	0.64995
CO <sub>2</sub>	0
H <sub>2</sub> S	0
CH <sub>4</sub>	3.3554E-06
NO <sub>x</sub>	0

Table 9. Output of Plant 201 (Stream 201S6)

Temperature F	200
Pressure psi	100
Vapor Frac	1
Mole Flow lbmol/hr	1.810E+5
Mass Flow lb/hr	2.075E+6
<b>Component</b>	<b>Mole Frac</b>
H <sub>2</sub>	0.621
N <sub>2</sub>	0.003
CO	0.328
CO <sub>2</sub>	0.003
H <sub>2</sub> O	0.044
CH <sub>4</sub>	Trace

In this base case, operating conditions of the Fischer-Tropsch synthesis were set to 525°K and 450 psi with the Co catalysts. For the other cases, only the parameter configuration of the F-T synthesis process (Plant 202) changed, while the parameter configurations of other plants remained the same. This allows examination of the effects of catalyst, temperature, and pressure on the products of the F-T conversion of coal to liquid fuels. Table 10 and Table 11 show the simulation results of Fischer-Tropsch synthesis plant (Plant 202) and Product Recovery Plant (Plant 203).

Table 10. Base Case Simulation Results – Properties of the Products

	Fuel Gas			Naphtha	Distillate	Wax
Component	C <sub>1</sub> -C <sub>4</sub> , H <sub>2</sub> , CO, CO <sub>2</sub> , H <sub>2</sub> O			C <sub>5</sub> -C <sub>10</sub>	C <sub>11</sub> -C <sub>19</sub>	C <sub>20+</sub>
Stream	203S9	203S10	203S11	203S12	203S13	202S14
Pressure psi	85	250	50	50	50	50
Temperature °F	200	0	100	100	100	100
Mass Flow lb/hr	4.532E+2	5.924E+5	2.878E+4	2.406E+5	1.827E+5	6.439E+4
Mole Flow lbmol/hr	2.379E+1	4.326E+4	6.065E+2	2.418E+3	9.686E+2	1.776E+2
Density lb/cuft	0.230	0.696	0.418	41.550	48.059	50.688

Table 11. Base Case Simulation Results - Product Selectivity

Component	WT %
C <sub>1</sub> -C <sub>4</sub>	20.45
C <sub>5</sub> -C <sub>10</sub>	39.28
C <sub>11</sub> -C <sub>19</sub>	28.30
C <sub>20+</sub>	10.19
Others	1.78
Total	100

The total amount of naphtha, distillate, and wax produced in this base case simulation was 4.876E+05 lb/hr. Using the input wet coal amount 2.537E+06lb/hr, 19.22% of the input coal was converted into products. Using dry coal, that conversion percentage was 29.57%. This percentage is an important factor in the efficiency of the coal to liquid fuels process.

### B. Case II – Catalyst Effect

The catalysts used in Fischer-Tropsch synthesis have a large effect on product selectivity. To examine the effects of the catalyst on the product selectivity of the F-T synthesis, Fe, Ru, and Ni catalysts are simulated individually at a temperature of 523°K and a pressure of 450 psi. Table 12 and Table 13 show the simulation results of catalyst effects on product amount and product selectivity.

Table 12. Simulation Results of Catalysts' Effect on Product Amount

Name		Fuel Gas			Naphtha	Distillate	Wax
Component		C <sub>1</sub> -C <sub>4</sub> , H <sub>2</sub> , CO, CO <sub>2</sub> , H <sub>2</sub> O			C <sub>5</sub> -C <sub>10</sub>	C <sub>11</sub> -C <sub>19</sub>	C <sub>20+</sub>
Stream		203S9	203S10	203S11	203S12	203S13	203S14
Mass Flow lb/hr	Fe	5.110E+2	5.159E+5	8.726E+3	1.108E+5	1.791E+5	2.974E+5
	Ru	5.465E+2	5.397E+5	1.368E+4	1.655E+5	2.061E+5	1.859E+5
	Ni	3.138E+1	7.241E+5	7.094E+4	2.447E+5	6.131E+4	2.837E+3
Mole Flow cuft/hr	Fe	2.993E+1	3.887E+4	1.992E+2	1.061E+3	8.903E+2	6.286E+2
	Ru	3.064E+1	4.021E+4	3.058E+2	1.613E+3	1.045E+3	4.426E+2
	Ni	1.506	4.919E+4	1.488E+3	2.638E+3	3.939E+2	9.052
Density lb/cuft	Fe	0.205	0.672	0.383	42.176	48.755	51.039
	Ru	0.215	0.680	0.392	41.937	48.518	50.844
	Ni	0.252	0.754	0.421	40.748	47.048	50.991

Table 13. Simulation Results of Catalysts' Effect on Product Selectivity

Catalyst Type	Co	Fe	Ru	Ni
C <sub>1</sub> -C <sub>4</sub> WT %	20.45	5.87	10.16	47.41
C <sub>5</sub> -C <sub>10</sub>	39.28	18.37	27.22	39.74
C <sub>11</sub> -C <sub>19</sub>	28.30	28.17	32.32	8.28
C <sub>20+</sub>	10.19	47.08	29.43	0.45

The total amount of naphtha, distillate, and wax produced in three simulations were 5.872E+05 lb/hr for Fe, 5.575E+05 lb/hr for Ru and 3.088E+05 for Ni. Thus, the coal conversion efficiency factor was 35.61% for Fe catalysts, 33.81% for Ru catalysts, and 18.72% for Ni catalysts on a dry coal basis.

At a temperature of 523°K and a pressure of 450 psi, Fe catalysts produced the highest molecular weight products and the largest C<sub>5+</sub> weight fraction, while Ni catalysts produced the lowest molecular weight and smallest C<sub>5+</sub> weight fraction.

### C. Case III – Temperature Effect

To examine the effects of temperature on the product selectivity of the F-T synthesis, several simulations were run with temperature ranging from 448°K to 648°K, using Co catalysts under a pressure of 450 psi.

Table 14. Simulation Results of Temperature's Effect on Product Selectivity

Temperature °K	473	498	523	548	598	648
C <sub>1</sub> -C <sub>4</sub> WT%	5.39	12.11	20.45	29.12	43.94	52.09
C <sub>5</sub> -C <sub>10</sub>	17.10	30.31	39.28	43.18	41.32	37.10
C <sub>11</sub> -C <sub>19</sub>	27.14	32.51	28.30	21.09	10.22	6.06
C <sub>20+</sub>	49.89	24.02	10.19	4.08	0.71	0.23
Others	0.47	1.05	1.78	2.53	3.82	4.53

Table 15. Simulation Results of Temperature's Effect on Amount of C<sub>5+</sub> Products and Conversion Efficiency Factor

Temperature °K	473	498	523	548	598	648
Mass Flow of C <sub>5+</sub> lb/hr	5.40E+5	5.44E+5	4.88E+5	4.32E+5	3.35E+5	2.83E+5
Conversion Efficiency %	32.75	32.75	29.57	26.20	26.20	26.20

Table 14 shows that temperature significantly influenced product selectivity. In general the F-T synthesis produced heavy products at low temperature while high temperature produced a lighter product distribution. Low temperature minimized the yields of light gas but generated a much greater yield of wax (C<sub>20+</sub>).

Table 15 shows that higher temperature produced less C<sub>5+</sub> products. At high temperature, most of the syngas was converted into light hydrocarbons with a carbon number less than 5. The total amount of Naphtha, distillates, and wax decreased, resulting in a decrease of the conversion efficiency of the whole coal to liquid fuels process.

#### D. Case IV – Pressure Effect

To examine the effects of pressure in the F-T synthesis, several simulations were run with pressures ranging from 100 psi to 700 psi using Co catalysts at a temperature of 523°K.

Table 16 and Table 17 show that generally higher pressure resulted in a heavier product distribution. The effect of pressure was reduced when the reactor pressure increased. Table 16 shows that higher pressure produced more C<sub>5+</sub> products. Because the volume contracts in the F-T synthesis, increasing reactor pressure increased the percentage of the CO converted in the reaction. Thus, the total amount of Naphtha, distillates, and wax increased, resulting in an increase of the conversion efficiency of the whole coal to liquid fuels process.

Table 16. Simulation Results of Pressure's Effect on Product Selectivity

Pressure psi	200	300	400	450	500	600	700
C <sub>1</sub> -C <sub>4</sub> WT %	45.59	33.97	27.11	22.35	20.45	18.78	15.97
C <sub>5</sub> -C <sub>10</sub>	37.24	43.57	42.67	40.54	39.28	37.96	35.23
C <sub>11</sub> -C <sub>19</sub>	12.63	17.13	22.80	26.80	28.30	29.53	31.26
C <sub>20+</sub>	0.57	2.38	5.07	8.37	10.19	12.11	16.15
Oxygenates	3.96	2.95	2.36	1.94	1.78	1.63	1.39

Table 17. Simulation Results of Pressure's Effect on Amount of C<sub>5+</sub> Products and Conversion Efficiency Factor

Pressure psi	200	300	400	450	500	600	700
Mass Flow of C <sub>5+</sub> lb/hr	3.38E+5	4.11E+5	4.66E+5	4.88E+5	5.10E+5	5.47E+5	5.79E+5
Conversion Efficiency %	20.48	24.91	28.26	29.57	30.95	33.19	35.11

This chapter described the steady-state behavior of the Fischer-Tropsch conversion of coal to liquid fuels process simulated by the ASPEN PLUS process flowsheet models. A base case and three other cases were simulated to study the effects of Fischer-Tropsch reaction conditions on F-T synthesis product selectivity. Simulation results were compared with the experimental results to examine the accuracy of user-defined model's (P202FT) predictions of F-T product selectivity. However, this study did not include detailed simulations to examine the reaction condition effects on the coal drying process, Shell gasification process, CO shift process, or hydrocarbon recovery process. All these processes were modeled by empirical models that concentrated on matching the reported composition and other physical properties of the main product streams from each process (e.g., temperature, pressure, and composition).

## VI. ECONOMICS

This chapter provides an economic estimate of the total capital investment to build a manufacturing complex using Fischer-Tropsch conversion of coal to liquid fuels. This economic estimate was based on the final report of "Baseline Design/Economics for Advanced Fischer-Tropsch Technology, Case 3–Wyoming Powder River Basin Coal with Conventional Refining Case" prepared by Bechtel Corporation. [25]

This estimate was based on a 2537.03 Mlbs/hr (30445 tons/day) wet coal input stream from Gillette, Wyoming. Some of the plants consist of several subsidiary plants that are combined together to estimate the amount of the capital investment. The Fischer-Tropsch conversion of coal to liquid fuels involves a variety of processes and nine major plants. The plants with \* are auxiliary plants and are not described in Chapter IV but are included in this economics study. Those auxiliary plants were not simulated in ASPEN PLUS software.

Table 18. Estimated Fixed Capital Investments

Plant	Description	Cost ( \$ Million)
101	Coal Drying Plant	199.84
102	Shell Gasification Plant	1139.79
103	Syngas Cooling & Cleanup Plant	332.46
104*	Coal Mining and Storage	73.89
105*	Air Separation Plant	474.96
201	CO Shift Plant	137.71
202	Fischer-Tropsch Synthesis Plant	541.26
203	Hydrocarbon Recovery	74.15
204*	Product Upgrading and Refining	217.84
Total		3191.90

The total capital cost of each plant consists of the ISBL (Inside Battery Limits) facilities cost, an apportioned allotment for the OSBL (Outside Battery Limits) plants, an amount for home office, engineering, and fees, and a contingency allotment. [9, 26] As shown at the bottom of the table, the total capital cost of the Fischer-Tropsch conversion of coal to liquid fuels at the Gillette, Wyoming, site will be about \$3.191 billion. The accuracy of this estimate is about +/- 30%, the same as that of the Wyoming Powder River Basin Coal with Conventional Refining Case.



## VII. DISCUSSION

The ASPEN PLUS process flowsheet models simulated the steady-state behavior of the Fischer-Tropsch conversion of coal to liquid fuels. Chapter IV discusses the effects of reaction conditions on F-T synthesis products selectivity. However, this study did not incorporate detailed simulations to examine the reaction condition effects on the coal drying process, Shell gasification process, CO shift process, or hydrocarbon recovery process. All these processes are modeled by empirical models that concentrate on matching the reported composition and other physical properties of the main product streams from each process (e.g., temperature, pressure, and composition).

The choice of catalysts for Fischer-Tropsch synthesis is a crucial element. Ni catalysts aren't ideal because they usually produce high amounts of methane and deteriorate rapidly when the pressure is higher than 1 atmosphere. Co catalysts have more desirable product selectivity than Ni catalysts and have been used more extensively. Ruthenium is an excellent catalyst at low temperature and high pressures for the production of very high molecular weight paraffins. The relative high costs of Co, Ru, and Ni catalysts promote continuous research on the development of Fe catalysts. One other advantage of Fe catalysts is their water-gas shift ability, eliminating the need for a CO Shift Plant and reducing capital investment. As a consequence, Fe catalysts are by far the most desirable catalysts for a large-scale commercial F-T process, and therefore, most of the current literature studies the Fe catalysts in Fischer-Tropsch synthesis.

Temperature also has a significant effect on F-T synthesis selectivity. As the temperature increases, the F-T selectivity moves towards the lower molecular mass products. There is an optimum temperature to maximize the selectivity of a certain range of products. For example, the maximum selectivity of naphtha ( $C_5$ - $C_{11}$ ) products occurs at about 275°C, while the maximum selectivity of the distillate ( $C_{12}$ - $C_{19}$ ) occurs at about 250°C.

A higher total pressure will result in a heavier F-T products distribution. The effect of the total pressure on product selectivity in the F-T synthesis is not directly related to the mechanism of the reaction. The partial pressure of reactants increases with the increasing total pressure, and it is the partial pressures of  $H_2$  and CO that govern the product selectivity [26]. On the other hand, pressure has a significant effect on the CO conversion percentage because there is a contraction in volume in the F-T synthesis.

There are deviations between the experimental results and the prediction of Fischer-Tropsch products selectivity. These errors derive from an approximation applied in the user-defined F-T synthesis model (P202FT) in the ASPEN PLUS



process flowsheet simulation. In this user-defined model, the base value of the chain growth probability  $\alpha$  of the catalysts is approximately the average value of that type of catalyst prepared by different methods. This gives a general prediction of F-T products selectivity of a certain catalyst type at certain points of temperature and pressure.

The errors also derive from another approximation applied in that user-defined model. The Anderson-Schultz-Flory distribution theory states that the moles of the F-T products show a linear relation with the carbon number on a semilogarithmic plot. An approximation of a factor of  $\text{CH}_2$  units (MW=14) is used to calculate the corresponding mass of the products. If the F-T synthesis products only consist of olefins, the user-defined model is 100% accurate. However, paraffins and oxygenates are formed in actual Fischer-Tropsch synthesis. Paraffins have almost the same molecular weight as olefins with carbon numbers larger than 4, while oxygenates' molecular weight is significantly larger than that of olefins. So the WT% of the F-T synthesis products with a certain carbon number range calculated from the model deviates from the experimental data.

In general, given reaction conditions, the APEN PLUS simulation model reasonably predicts the Fischer-Tropsch product selectivity, a main concern of the CAD design of the conversion of coal into liquid fuels.

On the scale of the whole coal to liquid fuels process, the major problems of Fischer-Tropsch conversion of coal to liquid fuels are well recognized. Most notably, the process design is complex. The whole process involves nine major plants requiring complicated equipment. This results in high capital investment costs and large operating expenses for maintenance. But without a doubt, the principle advantage of the Fischer-Tropsch process is its proven commercial success. As a result of reliability, there is a minimum of technological risk evolved. Another advantage is the flexibility of the process operating conditions (e.g., catalyst type, temperature, pressure) enabling a high degree of control over the final product composition. Furthermore, the final product fuels don't contain nitrogen and sulfur.

## VIII. CONCLUSIONS AND RECOMMENDATIONS FOR FUTURE WORK

### A. Conclusions

This study developed a conceptual design and ASPEN PLUS flowsheet simulation model for Fischer-Tropsch conversion of coal to liquid fuels. This model predicts the effects of the various process and operating changes on the overall plant heat and material balance with a focus on the effects of different Fischer-Tropsch synthesis operating conditions on the final product selectivity of the coal to liquid fuels process.

This process flowsheet simulation model is primarily a research guidance tool instead of a detailed process design tool. However, the model does contain some process design features. This model can be used to study the effects of Fischer-Tropsch synthesis operating conditions on the final yields of the coal to liquid fuels process. One can predict the pattern of the product distribution (Anderson-Shultz-Flory Law) under steady-state conditions using a simple model of the Fischer-Tropsch reaction involving chain growth kinetics by one carbon at a time. Given the operating conditions parameters, the ASPEN PLUS flowsheet simulation model can give a prediction of the final product yields and the utilities of the Fischer-Tropsch conversion of coal to liquid fuels process. Based on this information, a rough estimate of the capital investment can be obtained.

This model does not include detailed simulations of the syngas cooling and cleanup plant and hydrocarbon recovery plant. These plants are modeled by empirical models that concentrate on matching the reported composition of the main product streams of each plant. Starting with empirical models is standard procedure for any significant development project. As the project progresses and more data become available, the model then is enhanced and extended to add other features as desired. More detailed simulation models of these plants were not developed because such model development requires significant effort that was beyond the scope of this study.

### B. Recommendations for Future Work

Specific recommendations for possible future work include:

1. Extend the model of the Fischer-Tropsch synthesis plant to more rigorously represent the F-T synthesis product selectivity by incorporating a more accurate product distribution model into the user-defined model (P202FT). Some studies have indicated a dual chain growth probability mechanism in

Fischer-Tropsch synthesis, which can be developed and incorporated into the user-defined model to more accurately represent the F-T synthesis product distribution.

2. Extend the model of the syngas cooling and cleanup plant to represent the syngas cleanup process (a combination of an alkazid process, a carbon adsorption with subsequent  $(\text{NH}_4)_2\text{S}$  wash, and an iron oxide process) in more detail and predict the chemical consumption.
3. Develop a simplified yield ASPEN PLUS block model for a single hydroprocessing unit to process the Fischer-Tropsch synthesis products into a stable, transportable syncrude for further processing into finished products elsewhere.
4. Develop a detailed economics analysis of Fischer-Tropsch conversion of coal to liquid fuels based on the ASPEN PLUS process flowsheet simulation model developed in this study. This economics analysis is important to future F-T conversion coal to liquid fuels projects.
5. Develop processes for the production of synthetic liquid fuels with alternate feedstocks (natural gas, refinery by-product streams, bio-mass, etc.) based on the ASPEN PLUS flowsheet model developed in this thesis.

## IX. REFERENCES

1. World Energy Prospects to 2020, International Energy Agency, G8 Energy Ministers' Meeting, Moscow, 1998.
2. Coal Information, Kentucky Geological Survey, 2002.
3. U.S. Coal Production under the Surface Mining Law, 1978 – present, State of Wyoming, 1997.
4. The Fischer-Tropsch Synthesis, R.B Anderson, 1984.
5. Selectivity in Fischer-Tropsch Synthesis: Review and Recommendations for Future Work, L. Caldwell, Council for Scientific and Industrial Research, 1980.
6. Getting Started Building and Running a Process Model, Manual of Aspen Plus 11.1, Aspen Technology, Inc, 2002
7. Shell Gasification: Table 2-5: Coal Feed Analyses, Handbook of the Synfuels Technology, 1984.
8. The Shell Coal Gasification Process, E.V. Vogt, P.J. Weller and M.J. Vanderburgt, Handbook of the Synfuels Technology, 1984.
9. Topical Report: Aspen Process Flowsheet Simulation Model of a Battelle Biomass-Based Gasification, Fischer-Tropsch Liquefaction and Combined-Cycle Power Plant, Bechtel Corporation, Department of Energy, Contract No. DE-AC22-93PC91029-19, 1998
10. Kinetics and reaction Mechanism of The Fischer-Tropsch Synthesis, R.B. Anderson, Catalysis, Vol. 4, p. 350, 1956.
11. The Fischer-Tropsch and Related Synthesis, H.H. Storch, N. Golumbic and R.B. Anderson, 1951.
12. Conversion of Natural Gas To Transportation Fuels Via The Shell Middle Distillate Synthesis Process (SMDS), S.T. Sie, M.M.G. Senden and H.M.H. Van Wechem, Catalysis Today, Vol. 8, p371-394.,1991.

13. Proceeding of 9<sup>th</sup> International Congress on Catalysis, S.T. Sie, J. Eilers and J.K. Minderhoud, Chem. Inst. Canada, Vol. 2, p 743, 1988.
14. Technical Paper 709: Synthetic Liquid Fuels from Hydrogenation of Carbon Monoxide, Part 1. Review of Literature, Bureau of Mines, Department of Energy, H. H. Storch, R. B. Anderson, L. J. E. Hofer, C. O. Hawk, H. C. Anderson and N. Golumbic, 1948.
15. Middle Distillates from Syngas on Modified Cobalt Catalysts, P. Chaumette, C. Verdon, A. Kiennemann and S. Boujana, Preprints – Division of Petroleum Chemistry, American Chemical Society, Vol. 37, p833, 1992
16. Bifunctional Catalysts in Syngas Conversions, V. Udaya, S. Rao, Robert J. Gormley, Catalysis Today, Vol. 6, n3, p207, 1990.
17. Fischer-Tropsch Selectivity of Ni/Al<sub>2</sub>O<sub>3</sub> Catalysts, Hadjigeorghiou, G. A. and J.T. Richardson, Applied Catalysis, Vol. 21, n1, p11, 1986,
18. Bulletin 578: Synthetic Liquid from Hydrogenation of Carbon Monoxide, Bureau of Mines, Department of Energy, 1959.
19. Production of C<sub>4</sub> Hydrocarbons from Fischer-Tropsch Synthesis in a Follow bed Reactor Consisting of Co-Ni-ZrO<sub>2</sub> and Sulfated-ZrO<sub>2</sub> Catalyst beds, R. Sethuraman, N.N. Bakhshi, S.P. Katikaneni and R.O. Idem, Fuel Processing Technology, Vol. 73, p.197, 2001.
20. Fischer-Tropsch Reaction Studies with Supported Ruthenium Catalysts, R.C. Everson, E.T. Woodburn and A.R. Kirk, Journal of Catalysis, Vol. 53, 1978.
21. Iron-based Catalysts for Slurry-phase Fischer-Tropsch Process: Technology Review, V.U.S. Rao, G.J. Stiegel, G.J. Cinquegrane and R.D. Srivastava, Fuel Processing Technology, Vol. 30, 1992.
22. Proceeding 4<sup>th</sup> World Petroleum Congress, H. Kobel, P. Ackerman and F. Engelhardt, Section IV/C, p.227.1955

23. Final Report: Slurry Fischer-Tropsch/Mobil Two Stage Process of Converting Syngas to High Octane Gasoline, J.C.W. Kuo, Department of Energy, Contract No. DE-AC22-80PC30022, 1983.
24. Catalysts For Fischer-Tropsch, R.D. Srivastava, V.U.S. Rao, G. Cinquegrane and G.J. Stiegel, Hydrocarbon Processing, Vol. 69, p60, 1990.
25. The Influence of Kinetic Parameters on the Fischer-Tropsch Product Distribution, Jin Wang and B.W. Wojciechowski, Fuel Science and Technology, Vol. 7, p.1139, 1989.
26. Final Report: Baseline Design/Economics for Advanced Fischer-Tropsch Technology, Bechtel Corporation, Contract No. DE-AC22-91PC90027, Department of Energy, 1998.

## X. APPENDICES

### A. Input File Listing of the ASPEN PLUS Process Flowsheet Simulation Model of Section 1-Base Case

DYNAPLUS  
DPLUS RESULTS=ON

TITLE 'Section 1'

IN-UNITS ENG

DEF-STREAMS MCINCPSD ALL

DESCRIPTION "

Solids Simulation with English Units :  
F, psi, lb/hr, lbmol/hr, Btu/hr, cuft/hr.

Property Method: PENG-ROB

Flow basis for input: Mass  
"

DATABANKS PURE11 / AQUEOUS / SOLIDS / INORGANIC / &  
NOASPENPCD

PROP-SOURCES PURE11 / AQUEOUS / SOLIDS / INORGANIC

COMPONENTS

H2O H2O /  
N2 N2 /  
O2 O2 /  
COAL /  
NO2 NO2 /  
NO NO /  
S S /  
O2S O2S /  
SO3 O3S /  
H2 H2 /  
C C /  
CO CO /  
CO2 CO2 /

ASH /  
H2S H2S /  
CH4 CH4

FLOWSHEET

BLOCK P101B IN=101S1 OUT=101S2 101S3  
BLOCK P101A IN=WETCOAL N2 OUT=101S1  
BLOCK P102A IN=101S3 OUT=102S1  
BLOCK P102B IN=102S1 O2 OUT=102S2  
BLOCK P103H1 IN=103S1 WATER1 OUT=103S2 STEAM1  
BLOCK P103H2 IN=103S2 WATER2 OUT=103S3 STEAM2  
BLOCK P103C1 IN=102S3 OUT=103S1  
BLOCK P103S IN=103S4 103S3 OUT=103S5 103S6  
BLOCK P102C IN=102S2 OUT=ASH 102S3

PROPERTIES PENG-ROB  
PROPERTIES IDEAL

NC-COMPS COAL PROXANAL ULTANAL SULFANAL

NC-PROPS COAL ENTHALPY HCOALGEN 6 / DENSITY DCOALIGT

NC-COMPS ASH PROXANAL ULTANAL SULFANAL

NC-PROPS ASH ENTHALPY HCOALGEN / DENSITY DCOALIGT

PROP-DATA HEAT  
IN-UNITS ENG  
PROP-LIST HCOMB  
PVAL COAL 11700.

PROP-DATA PRKIJ-1  
IN-UNITS ENG  
PROP-LIST PRKIJ  
BPVAL H2O CO2 .1200000000  
BPVAL H2O H2S .0400000000  
BPVAL N2 CO2 -.0170000000  
BPVAL N2 H2S .1767000000  
BPVAL N2 O2 -.0119000000  
BPVAL N2 O2S .0800000000  
BPVAL N2 H2 .1030000000  
BPVAL N2 CO .0307000000  
BPVAL N2 CH4 .0311000000



BPVAL O2 N2 -.0119000000  
BPVAL O2S CH4 .1356000000  
BPVAL O2S N2 .0800000000  
BPVAL H2 CO2 -.1622000000  
BPVAL H2 CO .0919000000  
BPVAL H2 CH4 .0156000000  
BPVAL H2 N2 .1030000000  
BPVAL CO H2S .0544000000  
BPVAL CO H2 .0919000000  
BPVAL CO CH4 .0300000000  
BPVAL CO N2 .0307000000  
BPVAL CO2 H2S .0974000000  
BPVAL CO2 H2 -.1622000000  
BPVAL CO2 CH4 .0919000000  
BPVAL CO2 N2 -.0170000000  
BPVAL CO2 H2O .1200000000  
BPVAL H2S CO2 .0974000000  
BPVAL H2S CO .0544000000  
BPVAL H2S N2 .1767000000  
BPVAL H2S H2O .0400000000  
BPVAL CH4 CO2 .0919000000  
BPVAL CH4 O2S .1356000000  
BPVAL CH4 H2 .0156000000  
BPVAL CH4 CO .0300000000  
BPVAL CH4 N2 .0311000000

DEF-STREAMS CONVEN WATER1 STEAM1 STEAM2 103S3 103S1  
WATER2 &  
103S4 103S5 103S6 103S2

DEF-STREAMS MCINCPSD 102S3

PROP-SET ALL-SUBS VOLFLMX MASSVFRA MASSSFRA RHOMX  
MASSFLOW &  
TEMP PRES UNITS='lb/cuft' SUBSTREAM=ALL  
; "Entire Stream Flows, Density, Phase Frac, T, P"

STREAM 103S4  
SUBSTREAM MIXED TEMP=70. PRES=14.7 MOLE-FLOW=20.  
MOLE-FRAC H2O 1.

STREAM N2

SUBSTREAM MIXED TEMP=450. PRES=14.7 MASS-FLOW=7500.  
<Mlb/hr>  
MOLE-FRAC N2 0.9999 / O2 0.0001

STREAM O2  
SUBSTREAM MIXED TEMP=77. PRES=14.7 MASS-FLOW=1875.  
<Mlb/hr>  
MOLE-FRAC N2 0.001 / O2 0.999

STREAM WATER1  
SUBSTREAM MIXED TEMP=70. PRES=14.7 MASS-FLOW=750. <Mlb/hr>  
MASS-FRAC H2O 1.

STREAM WATER2  
SUBSTREAM MIXED TEMP=70. PRES=14.7 MASS-FLOW=850. <Mlb/hr>  
MASS-FRAC H2O 1.

STREAM WETCOAL  
SUBSTREAM NCPSD TEMP=77. PRES=14.7 &  
MASS-FLOW=2537.034 <Mlb/hr>  
MASS-FLOW COAL 2537.034 <Mlb/hr>  
COMP-ATTR COAL PROXANAL ( 35. 47.4 46.7 5.9 )  
COMP-ATTR COAL ULTANAL ( 5.9 75.6 6. 0.7 0. 0.9 16.8 )  
COMP-ATTR COAL SULFANAL ( 0.4 0.1 0.4 )  
SUBS-ATTR PSD ( 0 0 0.1 0.3 0.4 0.2 )

BLOCK P102C SEP  
PARAM  
FRAC STREAM=ASH SUBSTREAM=MIXED COMPS=H2O N2 O2 NO2  
NO &  
S O2S SO3 H2 C CO CO2 H2S CH4 FRACS=0. 0. 0. 0. &  
0. 0. 0. 0. 0. 1. 0. 0. 0. 0.  
FRAC STREAM=ASH SUBSTREAM=CIPSD COMPS=C FRACS=1.  
FRAC STREAM=ASH SUBSTREAM=NCPSD COMPS=COAL ASH  
FRACS=1. &  
1.  
FLASH-SPECS 102S3 TEMP=1500. <C> PRES=430.

BLOCK P103S SEP  
PARAM  
FRAC STREAM=103S5 SUBSTREAM=MIXED COMPS=H2O N2 O2 NO2  
&  
NO S O2S SO3 H2 C CO CO2 H2S CH4 FRACS=0.8 1. 0. &

0. 0. 0. 0. 0. 1. 0. 1. 0. 0. 1.  
FLASH-SPECS 103S6 PRES=14.7 NPHASE=1 FREE-WATER=NO  
PHASE=L  
FLASH-SPECS 103S5 TEMP=100. PRES=130. NPHASE=1 &  
FREE-WATER=NO PHASE=V

BLOCK P101B FLASH2  
PARAM PRES=14.7 DUTY=0.

BLOCK P103H1 HEATX  
PARAM T-COLD=750. CALC-TYPE=DESIGN PRES-COLD=975. &  
U-OPTION=PHASE F-OPTION=CONSTANT CALC-  
METHOD=SHORTCUT  
FEEDS HOT=103S1 COLD=WATER1  
PRODUCTS HOT=103S2 COLD=STEAM1  
HOT-SIDE DP-OPTION=CONSTANT  
COLD-SIDE DP-OPTION=CONSTANT

BLOCK P103H2 HEATX  
PARAM T-COLD=530. CALC-TYPE=DESIGN PRES-HOT=130. &  
PRES-COLD=530. U-OPTION=CONSTANT F-OPTION=CONSTANT &  
CALC-METHOD=SHORTCUT  
FEEDS HOT=103S2 COLD=WATER2  
PRODUCTS HOT=103S3 COLD=STEAM2  
HOT-SIDE DP-OPTION=CONSTANT  
COLD-SIDE DP-OPTION=CONSTANT

BLOCK P101A RSTOIC  
PARAM PRES=14.7 DUTY=0.  
STOIC 1 NCPSD COAL -1. / MIXED H2O 0.0555084  
CONV 1 NCPSD COAL 0.2  
COMP-ATTR NCPSD COAL PROXANAL ( 20. )

BLOCK P102A RYIELD  
PARAM TEMP=77. PRES=14.7  
MASS-YIELD MIXED H2O 0.1 / NCPSD ASH 0.2 / CIPSD C &  
0.1 / MIXED H2 0.1 / N2 0.2 / S 0.1 / O2 0.1  
COMP-ATTR NCPSD ASH SULFANAL ( 0. 0. 0. )  
COMP-ATTR NCPSD ASH ULTANAL ( 100. 0. 0. 0. 0. 0. 0. &  
)  
COMP-ATTR NCPSD ASH PROXANAL ( 0. 0. 0. 100. )  
SUBS-ATTR 1 CIPSD PSD ( 0 0 0.1 0.3 0.4 0.2 )  
SUBS-ATTR 2 NCPSD PSD ( 0 0 0.1 0.2 0.4 0.2 0.1 )

BLOCK P102B RGIBBS  
PARAM TEMP=2000. <C> PRES=430.  
PROD H2O / H2 / CO / CO2 / C SS / N2 / H2S / O2S / &  
SO3 / NO2 / NO / CH4

BLOCK P103C1 CLCHNG

EO-CONV-OPTI

CALCULATOR C-1

DEFINE H2OIN COMP-ATTR-VAR STREAM=WETCOAL  
SUBSTREAM=NCPSD &  
COMPONENT=COAL ATTRIBUTE=PROXANAL ELEMENT=1  
DEFINE H2ODRY BLOCK-VAR BLOCK=P101A VARIABLE=VALUE &  
SENTENCE=COMP-ATTR ID1=1 ELEMENT=1  
DEFINE CONV BLOCK-VAR BLOCK=P101A VARIABLE=CONV &  
SENTENCE=CONV ID1=1  
F H2ODRY=2.0  
F CONV=(H2OIN-H2ODRY)/(100-H2ODRY)  
EXECUTE BEFORE BLOCK P101A

CALCULATOR C-2

VECTOR-DEF ULT COMP-ATTR STREAM=101S3 SUBSTREAM=NCPSD  
&  
COMPONENT=COAL ATTRIBUTE=ULTANAL  
DEFINE WATER COMP-ATTR-VAR STREAM=101S3  
SUBSTREAM=NCPSD &  
COMPONENT=COAL ATTRIBUTE=PROXANAL ELEMENT=1  
DEFINE H2O BLOCK-VAR BLOCK=P102A VARIABLE=YIELD &  
SENTENCE=MASS-YIELD ID1=MIXED ID2=H2O  
DEFINE ASH BLOCK-VAR BLOCK=P102A VARIABLE=YIELD &  
SENTENCE=MASS-YIELD ID1=NCPSD ID2=ASH  
DEFINE CARB BLOCK-VAR BLOCK=P102A VARIABLE=YIELD &  
SENTENCE=MASS-YIELD ID1=CIPSD ID2=C  
DEFINE H2 BLOCK-VAR BLOCK=P102A VARIABLE=YIELD &  
SENTENCE=MASS-YIELD ID1=MIXED ID2=H2  
DEFINE N2 BLOCK-VAR BLOCK=P102A VARIABLE=YIELD &  
SENTENCE=MASS-YIELD ID1=MIXED ID2=N2  
DEFINE SULF BLOCK-VAR BLOCK=P102A VARIABLE=YIELD &  
SENTENCE=MASS-YIELD ID1=MIXED ID2=S  
DEFINE O2 BLOCK-VAR BLOCK=P102A VARIABLE=YIELD &  
SENTENCE=MASS-YIELD ID1=MIXED ID2=O2  
C FACT IS THE FACTOR TO CONVERT

```

F FACT=(100-WATER)/100
F H2O=WATER/100
F ASH=ULT(1)/100*FACT
F CARB=ULT(2)/100*FACT
F H2=ULT(3)/100*FACT
F N2=ULT(4)/100*FACT
F SULF=ULT(6)/100*FACT
F O2=1-H2O-ASH-CARB-H2-N2-CL2-SULF
EXECUTE BEFORE BLOCK P102A

```

### CALCULATOR C-3

```

DEFINE NAOH STREAM-VAR STREAM=103S4 SUBSTREAM=MIXED
&
  VARIABLE=MOLE-FLOW
DEFINE H2S MOLE-FLOW STREAM=103S1 SUBSTREAM=MIXED &
  COMPONENT=H2S
DEFINE SO2 MOLE-FLOW STREAM=103S1 SUBSTREAM=MIXED &
  COMPONENT=O2S
DEFINE SO3 MOLE-FLOW STREAM=103S1 SUBSTREAM=MIXED &
  COMPONENT=SO3
DEFINE NO2 MOLE-FLOW STREAM=103S1 SUBSTREAM=MIXED &
  COMPONENT=NO2
DEFINE CO2 MOLE-FLOW STREAM=103S1 SUBSTREAM=MIXED &
  COMPONENT=CO2
F NAOH=2*(SO2+CO2+NO2+SO3+H2S)
EXECUTE BEFORE BLOCK P103S

```

```

STREAM-REPOR NOZEROFLOW MOLEFLOW MASSFLOW MOLEFRAC
NOATTR-DESC &
  NOCOMP-ATTR NOSUBS-ATTR PROPERTIES=ALL-SUBS

```

```
PROPERTY-REP NOPARAM-PLUS
```

### B. Input File Listing of the ASPEN PLUS Process Flowsheet Simulation Model of Section 2-Base Case

```

DYNAPLUS
DPLUS RESULTS=ON

```

```

TITLE 'Section 2'
IN-UNITS ENG
DEF-STREAMS CONVEN ALL

```

## SIM-OPTIONS

IN-UNITS ENG MOLE-FLOW=MMscfd VOLUME-FLOW='MMcuft/hr' &  
ENTHALPY-FLO='MMBtu/hr' HEAD=ft MOLES=MMscf HEAT=MMBtu  
SIM-OPTIONS NPHASE=2

## DESCRIPTION "

Gas Processing with English Units:  
F, psi, lb/hr, MMscfd, MMBtu/hr, MMcuft/hr.

Property Method: PENG-ROB

Flow basis for input: Mole

Stream report composition: Mole flow  
"

DATABANKS PURE11 / ASPENPCD

PROP-SOURCES PURE11 / ASPENPCD

## COMPONENTS

H2 H2 /  
N2 N2 /  
CO CO /  
CO2 CO2 /  
H2O H2O /  
CH4 CH4 /  
C2H4 C2H4 /  
C2H6 C2H6 /  
C3H6 C3H6-2 /  
C3H8 C3H8 /  
NC4H8 C4H8-1 /  
NC4H10 C4H10-1 /  
C5H10 C5H10-2 /  
NC5H12 C5H12-1 /  
C6H12 C6H12-3 /  
NC6H14 C6H14-1 /  
C7H14 C7H14-7 /  
C7H16-1 C7H16-1 /  
C8H16 C8H16-16 /  
C8H18-1 C8H18-1 /  
C9H18-3 C9H18-3 /

C9H20-1 C9H20-1 /  
C10H20-5 C10H20-5 /  
C10H22-1 C10H22-1 /  
C11H22-2 C11H22-2 /  
C11H24 C11H24 /  
C12H24-2 C12H24-2 /  
C12H26 C12H26 /  
C13H26-2 C13H26-2 /  
C13H28 C13H28 /  
C14H28-2 C14H28-2 /  
C14H30 C14H30 /  
C15H30-2 C15H30-2 /  
C15H32 C15H32 /  
C16H32-2 C16H32-2 /  
C16H34 C16H34 /  
C17H34 C17H34-D1 /  
C17H36 C17H36 /  
C18H36-1 C18H36-1 /  
C18H38 C18H38 /  
C19H38 C19H38-D1 /  
C19H40 C19H40 /  
C20H40 C20H40-D1 /  
C20H42 C20H42 /  
OXVAP C2H6O-2 /  
OXHC C5H12O-1 /  
OXH2O C2H6O-2 /  
C10AP C10H14-1 /  
C21OP /  
C22OP /  
C23OP /  
C24OP /  
C25OP /  
C26OP /  
C27OP /  
C28OP /  
C29OP /  
C30WAX

PC-USER

IN-UNITS ENG MOLE-FLOW=MMscfd VOLUME-FLOW='MMcuft/hr' &  
ENTHALPY-FLO='MMBtu/hr' HEAD=ft MOLES=MMscf HEAT=MMBtu  
PC-DEF API-METH C21OP NBP=672.2 API=45.24 MW=295.1675  
PC-DEF API-METH C22OP NBP=694.2 API=44.68 MW=309.1943

PC-DEF API-METH C23OP NBP=715.3 API=44.23 MW=323.2211  
PC-DEF API-METH C24OP NBP=735.4 API=43.83 MW=337.2479  
PC-DEF API-METH C25OP NBP=754.6 API=43.45 MW=351.2747  
PC-DEF API-METH C26OP NBP=773.4 API=43.07 MW=365.3015  
PC-DEF API-METH C27OP NBP=791.2 API=42.69 MW=379.3283  
PC-DEF API-METH C28OP NBP=808.4 API=42.42 MW=393.3354  
PC-DEF API-METH C29OP NBP=825. API=41.87 MW=407.3891  
PC-DEF API-METH C30WAX NBP=974.3 API=36.42 MW=742.6992

#### ADA-SETUP

ADA-SETUP PROCEDURE=REL9

#### FLWSHEET

BLOCK P202S IN=202S2 OUT=202S4 202S3  
BLOCK P203S1 IN=203S1 OUT=203S4 203S5  
BLOCK P203S2 IN=203S3 OUT=203S9 203S7  
BLOCK P203S4 IN=203S6 203S7 OUT=203S11 203S13 203S14 &  
203S15 203S12  
BLOCK P203S3 IN=203S4 OUT=203S10 203S6  
BLOCK P202FT IN=202S1 OUT=202S2  
BLOCK P202C IN=201S6 OUT=202S1  
BLOCK P201A IN=201S1 STEAM OUT=201S2 201S3  
BLOCK P201H1 IN=SYNGAS OUT=201S1  
BLOCK P201H2 IN=201S2 OUT=201S4  
BLOCK P201S IN=201S4 OUT=201S6 201S5  
BLOCK P203H1 IN=202S4 OUT=203S1  
BLOCK P203H2 IN=202S3 OUT=203S3 203S2

#### PROPERTIES PENG-ROB

#### PROP-DATA PURE-1

IN-UNITS ENG MOLE-FLOW=MMscfd VOLUME-FLOW='MMcuft/hr' &  
ENTHALPY-FLO='MMBtu/hr' HEAD=ft MOLE-ENTHALP='J/kmol' &  
MOLES=MMscf HEAT=MMBtu  
PROP-LIST DGFORM / DHFORM  
PVAL C21OP 1.831E+8 / -3.909E+8  
PVAL C22OP 1.912E+8 / -4.129E+8  
PVAL C23OP 1.982E+8 / -4.352E+8  
PVAL C24OP 2.061E+8 / -4.581E+8  
PVAL C25OP 2.127E+8 / -5.051E+8  
PVAL C26OP 2.204E+8 / -5.293E+8  
PVAL C27OP 2.273E+8 / -5.540E+8  
PVAL C28OP 2.341E+8 / -5.791E+8



PVAL C29OP 2.407E+8 / -6.047E+8  
PVAL C30WAX 4.082E+8 / -1.217E+9  
PVAL OXVAP -1.948E+8 / -2.727E+8  
PVAL OXHC -1.555E+8 / -3.185E+8  
PVAL OXH2O -1.710E+8 / -2.393E+8  
PVAL C10AP 1.5358E+8 / -3.3810E+7

PROP-DATA PURE-2

IN-UNITS ENG  
PROP-LIST MW  
PVAL H2 2.0158  
PVAL N2 28.0134  
PVAL CO 28.0104  
PVAL CO2 44.0098  
PVAL H2O 18.0152  
PVAL CH4 16.0426  
PVAL C2H4 28.0536  
PVAL C2H6 30.0694  
PVAL C3H6 42.0804  
PVAL C3H8 44.0962  
PVAL NC4H8 56.1072  
PVAL NC4H10 58.1230  
PVAL C5H10 70.134  
PVAL NC5H12 72.1498  
PVAL C6H12 84.1608  
PVAL NC6H14 86.1766  
PVAL C7H14 98.1876  
PVAL C7H16-1 100.2034  
PVAL C8H16 112.2144  
PVAL C8H18-1 114.2302  
PVAL C9H18-3 126.2412  
PVAL C9H20-1 128.2570  
PVAL C10H20-5 140.2680  
PVAL C10H22-1 142.2838  
PVAL C11H22-2 154.2948  
PVAL C11H24 156.3106  
PVAL C12H24-2 168.3216  
PVAL C12H26 170.3374  
PVAL C13H26-2 182.3484  
PVAL C13H28 184.3642  
PVAL C14H28-2 196.3752  
PVAL C14H30 198.3910  
PVAL C15H30-2 210.4020

PVAL C15H32 212.4178  
PVAL C16H32-2 224.4288  
PVAL C16H34 226.4446  
PVAL C17H34 238.4556  
PVAL C17H36 240.4714  
PVAL C18H36-1 252.4824  
PVAL C18H38 254.4982  
PVAL C19H38 266.5092  
PVAL C19H40 268.5250  
PVAL C20H40 280.5360  
PVAL C20H42 282.5518

PROP-DATA ATOMNO-1

IN-UNITS ENG MOLE-FLOW=MMscfd VOLUME-FLOW='MMcuft/hr' &  
ENTHALPY-FLO='MMBtu/hr' HEAD=ft MOLES=MMscf HEAT=MMBtu

PROP-LIST ATOMNO

PVAL C30WAX 6 1 8  
PVAL OXVAP 6 1 8  
PVAL OXHC 6 1 8  
PVAL OXH2O 6 1 8  
PVAL C21OP 6 1 8  
PVAL C22OP 6 1 8  
PVAL C23OP 6 1 8  
PVAL C24OP 6 1 8  
PVAL C25OP 6 1 8  
PVAL C26OP 6 1 8  
PVAL C27OP 6 1 8  
PVAL C28OP 6 1 8  
PVAL C29OP 6 1 8

PROP-DATA NOATOM-1

IN-UNITS ENG MOLE-FLOW=MMscfd VOLUME-FLOW='MMcuft/hr' &  
ENTHALPY-FLO='MMBtu/hr' HEAD=ft MOLES=MMscf HEAT=MMBtu

PROP-LIST NOATOM

PVAL C30WAX 52.524 105.648 0.335  
PVAL OXVAP 2.43 5.69 1.00  
PVAL OXHC 4.78 11.14 1.10  
PVAL OXH2O 1.95 5.77 1.02  
PVAL C21OP 21 42.6 0  
PVAL C22OP 22 44.6 0  
PVAL C23OP 23 46.6 0  
PVAL C24OP 24 48.6 0  
PVAL C25OP 25 50.6 0

PVAL C26OP 26 52.6 0  
PVAL C27OP 27 54.6 0  
PVAL C28OP 28 56.6 0  
PVAL C29OP 29 58.6 0

PROP-DATA PRKIJ-1

IN-UNITS ENG MOLE-FLOW=MMscfd VOLUME-FLOW='MMcuft/hr' &  
ENTHALPY-FLO='MMBtu/hr' HEAD=ft MOLES=MMscf HEAT=MMBtu

PROP-LIST PRKIJ

BPVAL C2H4 C2H6 8.90000000E-3  
BPVAL C2H4 NC4H10 .0922000000  
BPVAL C2H4 H2 7.40000000E-3  
BPVAL C2H4 N2 .0856000000  
BPVAL C2H4 CO2 .0552000000  
BPVAL C2H4 CH4 .0215000000  
BPVAL C2H4 C7H16-1 .0144000000  
BPVAL C2H6 NC4H10 9.60000000E-3  
BPVAL C2H6 H2 -.0667000000  
BPVAL C2H6 N2 .0515000000  
BPVAL C2H6 CO2 .1322000000  
BPVAL C2H6 CH4 -2.60000000E-3  
BPVAL C2H6 C7H16-1 6.70000000E-3  
BPVAL C2H6 C2H4 8.90000000E-3  
BPVAL C2H6 C3H8 1.10000000E-3  
BPVAL C2H6 C3H6 8.90000000E-3  
BPVAL C2H6 CO -.0226000000  
BPVAL C2H6 NC5H12 7.80000000E-3  
BPVAL C2H6 NC6H14 -.0100000000  
BPVAL C2H6 C8H18-1 .0185000000  
BPVAL C3H8 C2H6 1.10000000E-3  
BPVAL C3H8 NC4H10 3.30000000E-3  
BPVAL C3H8 H2 -.0833000000  
BPVAL C3H8 N2 .0852000000  
BPVAL C3H8 CO2 .1241000000  
BPVAL C3H8 CH4 .0140000000  
BPVAL C3H8 C7H16-1 5.60000000E-3  
BPVAL C3H8 C3H6 7.40000000E-3  
BPVAL C3H8 CO .0259000000  
BPVAL C3H8 NC5H12 .0267000000  
BPVAL C3H8 NC6H14 7.00000000E-4  
BPVAL C3H8 OXVAP .0315000000  
BPVAL C3H8 OXH2O .0315000000  
BPVAL C3H6 C2H6 8.90000000E-3

BPVAL C3H6 H2 -.1037000000  
BPVAL C3H6 N2 .0900000000  
BPVAL C3H6 CO2 .0933000000  
BPVAL C3H6 CH4 .0330000000  
BPVAL C3H6 C3H8 7.40000000E-3  
BPVAL C3H6 NC4H8 4.00000000E-4  
BPVAL NC4H8 NC4H10 1.10000000E-3  
BPVAL NC4H8 CO2 .0593000000  
BPVAL NC4H8 C3H6 4.00000000E-4  
BPVAL NC4H10 C2H6 9.60000000E-3  
BPVAL NC4H10 H2 -.3970000000  
BPVAL NC4H10 N2 .0800000000  
BPVAL NC4H10 CO2 .1333000000  
BPVAL NC4H10 CH4 .0133000000  
BPVAL NC4H10 C7H16-1 3.30000000E-3  
BPVAL NC4H10 C2H4 .0922000000  
BPVAL NC4H10 C3H8 3.30000000E-3  
BPVAL NC4H10 NC5H12 .0174000000  
BPVAL NC4H10 NC6H14 -5.60000000E-3  
BPVAL NC4H10 NC4H8 1.10000000E-3  
BPVAL H2 C2H6 -.0667000000  
BPVAL H2 NC4H10 -.3970000000  
BPVAL H2 N2 .1030000000  
BPVAL H2 CO2 -.1622000000  
BPVAL H2 CH4 .0156000000  
BPVAL H2 C7H16-1 -.1167000000  
BPVAL H2 C2H4 7.40000000E-3  
BPVAL H2 C3H8 -.0833000000  
BPVAL H2 C3H6 -.1037000000  
BPVAL H2 CO .0919000000  
BPVAL H2 NC6H14 -.0300000000  
BPVAL N2 C2H6 .0515000000  
BPVAL N2 NC4H10 .0800000000  
BPVAL N2 H2 .1030000000  
BPVAL N2 CO2 -.0170000000  
BPVAL N2 CH4 .0311000000  
BPVAL N2 C7H16-1 .1441000000  
BPVAL N2 C2H4 .0856000000  
BPVAL N2 C3H8 .0852000000  
BPVAL N2 C3H6 .0900000000  
BPVAL N2 CO .0307000000  
BPVAL N2 NC5H12 .1000000000  
BPVAL N2 NC6H14 .1496000000

BPVAL N2 C8H18-1 -.4100000000  
BPVAL CO C2H6 -.0226000000  
BPVAL CO H2 .0919000000  
BPVAL CO N2 .0307000000  
BPVAL CO CH4 .0300000000  
BPVAL CO C3H8 .0259000000  
BPVAL CO2 C2H6 .1322000000  
BPVAL CO2 NC4H10 .1333000000  
BPVAL CO2 H2 -.1622000000  
BPVAL CO2 N2 -.0170000000  
BPVAL CO2 CH4 .0919000000  
BPVAL CO2 C7H16-1 .1000000000  
BPVAL CO2 C2H4 .0552000000  
BPVAL CO2 C3H8 .1241000000  
BPVAL CO2 C3H6 .0933000000  
BPVAL CO2 NC5H12 .1222000000  
BPVAL CO2 NC6H14 .1100000000  
BPVAL CO2 NC4H8 .0593000000  
BPVAL CO2 H2O .1200000000  
BPVAL H2O CO2 .1200000000  
BPVAL CH4 C2H6 -2.6000000E-3  
BPVAL CH4 NC4H10 .0133000000  
BPVAL CH4 H2 .0156000000  
BPVAL CH4 N2 .0311000000  
BPVAL CH4 CO2 .0919000000  
BPVAL CH4 C7H16-1 .0352000000  
BPVAL CH4 C2H4 .0215000000  
BPVAL CH4 C3H8 .0140000000  
BPVAL CH4 C3H6 .0330000000  
BPVAL CH4 CO .0300000000  
BPVAL CH4 NC5H12 .0230000000  
BPVAL CH4 NC6H14 .0422000000  
BPVAL CH4 C8H18-1 .0496000000  
BPVAL CH4 C9H20-1 .0474000000  
BPVAL NC5H12 C2H6 7.80000000E-3  
BPVAL NC5H12 NC4H10 .0174000000  
BPVAL NC5H12 N2 .1000000000  
BPVAL NC5H12 CO2 .1222000000  
BPVAL NC5H12 CH4 .0230000000  
BPVAL NC5H12 C7H16-1 7.40000000E-3  
BPVAL NC5H12 C3H8 .0267000000  
BPVAL NC5H12 C8H18-1 0.0  
BPVAL NC6H14 C2H6 -.0100000000

BPVAL NC6H14 NC4H10 -5.6000000E-3  
 BPVAL NC6H14 H2 -.0300000000  
 BPVAL NC6H14 N2 .1496000000  
 BPVAL NC6H14 CO2 .1100000000  
 BPVAL NC6H14 CH4 .0422000000  
 BPVAL NC6H14 C7H16-1 -7.8000000E-3  
 BPVAL NC6H14 C3H8 7.00000000E-4  
 BPVAL NC6H14 OXHC .0456000000  
 BPVAL C7H16-1 C2H6 6.70000000E-3  
 BPVAL C7H16-1 NC4H10 3.30000000E-3  
 BPVAL C7H16-1 H2 -.1167000000  
 BPVAL C7H16-1 N2 .1441000000  
 BPVAL C7H16-1 CO2 .1000000000  
 BPVAL C7H16-1 CH4 .0352000000  
 BPVAL C7H16-1 C2H4 .0144000000  
 BPVAL C7H16-1 C3H8 5.60000000E-3  
 BPVAL C7H16-1 NC5H12 7.40000000E-3  
 BPVAL C7H16-1 NC6H14 -7.8000000E-3  
 BPVAL C8H18-1 C2H6 .0185000000  
 BPVAL C8H18-1 N2 -.4100000000  
 BPVAL C8H18-1 CH4 .0496000000  
 BPVAL C8H18-1 NC5H12 0.0  
 BPVAL C9H20-1 CH4 .0474000000  
 BPVAL OXVAP C3H8 .0315000000  
 BPVAL OXH2O C3H8 .0315000000  
 BPVAL OXHC NC6H14 .0456000000

PROP-SET GASPROPS

IN-UNITS ENG MOLE-FLOW=MMscfd VOLUME-FLOW='MMcuft/hr' &  
 ENTHALPY-FLO='MMBtu/hr' HEAD=ft MOLES=MMscf HEAT=MMBtu  
 PROPNAME-LIS ZMX VMX MOLEFLMX CPCVMX UNITS='cuft/min' &  
 'MMscfd' SUBSTREAM=MIXED PHASE=V;  
 "Compressibility, volume flow, heat capacity ratio"

STREAM STEAM

SUBSTREAM MIXED TEMP=430. PRES=360.  
 MOLE-FLOW H2O 4.2 <kmol/sec>

STREAM SYNGAS

IN-UNITS ENG MOLE-FLOW=MMscfd VOLUME-FLOW='MMcuft/hr' &  
 ENTHALPY-FLO='MMBtu/hr' HEAD=ft MOLES=MMscf HEAT=MMBtu

SUBSTREAM MIXED TEMP=100. PRES=130. FREE-WATER=NO  
NPHASE=1 &  
PHASE=V  
MOLE-FLOW H2 6.597824281 <kmol/sec> / N2 &  
0.068600234 <kmol/sec> / CO 15.04311445 <kmol/sec> / &  
H2O 1.435102473 <kmol/sec> / CH4 7.76589E-005 <kmol/sec>

BLOCK P201S SEP

PARAM  
FRAC STREAM=201S6 SUBSTREAM=MIXED COMPS=H2 N2 CO CO2 &  
H2O CH4 FRACS=1. 1. 1. 0.01 1. 1.  
FLASH-SPECS 201S6 TEMP=200. NPHASE=1 FREE-WATER=NO  
PHASE=V  
FLASH-SPECS 201S5 TEMP=70. PRES=14.7

BLOCK P203S1 SEP

PARAM  
FRAC STREAM=203S4 SUBSTREAM=MIXED COMPS=H2 N2 CO CO2 &  
H2O CH4 C2H4 C2H6 C3H6 C3H8 NC4H8 NC4H10 C5H10 &  
NC5H12 C6H12 NC6H14 C7H14 C7H16-1 C8H16 C8H18-1 &  
C9H18-3 C9H20-1 C10H20-5 C10H22-1 C11H22-2 C11H24 &  
C12H24-2 C12H26 C13H26-2 C13H28 C14H28-2 C14H30 &  
C15H30-2 C15H32 C16H32-2 C16H34 C17H34 C17H36 C18H36-1 &  
C18H38 C19H38 C19H40 C20H40 C20H42 OXVAP OXHC OXH2O &  
C10AP C21OP C22OP C23OP C24OP C25OP C26OP C27OP C28OP &  
C29OP C30WAX FRACS=1. 1. 1. 0.8 0. 1. 1. 1. 1. 1. &  
1. 1. 1. 1. 1. 1. 1. 1. 1. 1. 1. 1. 1. 1. 1. &  
1. 1. 1. 1. 1. 1. 1. 1. 1. 1. 1. 1. 1. 1. 1. &  
1. 1. 1. 1. 0. 1. 0. 1. 1. 1. 1. 1. 1. 1. 1. 1. &  
1. 1. 1.  
FLASH-SPECS 203S4 TEMP=70. PRES=250. NPHASE=1 FREE-  
WATER=NO &  
PHASE=V  
FLASH-SPECS 203S5 TEMP=70. PRES=50. NPHASE=1 FREE-WATER=NO  
&  
PHASE=L

BLOCK P203S4 SEP

PARAM PRES=100. NPHASE=2  
FRAC STREAM=203S11 SUBSTREAM=MIXED COMPS=H2 N2 CO CO2  
&  
H2O CH4 C2H4 C2H6 C3H6 C3H8 NC4H8 NC4H10 C5H10 &  
NC5H12 OXVAP FRACS=1. 1. 1. 0.3 0.15 1. 1. 1. 1. &

1. 1. 1. 0.12742 0.0596 1.  
 FRAC STREAM=203S13 SUBSTREAM=MIXED COMPS=CO2 H2O  
 C11H22-2 &  
 C11H24 C12H24-2 C12H26 C13H26-2 C13H28 C14H28-2 C14H30 &  
 C15H30-2 C15H32 C16H32-2 C16H34 C17H34 C17H36 C18H36-1 &  
 C18H38 C19H38 C19H40 OXHC FRACS=0. 0. 1. 1. 1. 1. &  
 1. 1. 1. 1. 1. 1. 1. 1. 1. 1. 1. 1. 0.52  
 FRAC STREAM=203S14 SUBSTREAM=MIXED COMPS=CO2 H2O  
 C20H40 &  
 C20H42 C21OP C22OP C23OP C24OP C25OP C26OP C27OP &  
 C28OP C29OP C30WAX FRACS=0. 0. 1. 1. 1. 1. 1. 1. &  
 1. 1. 1. 1. 1. 1.  
 FRAC STREAM=203S12 SUBSTREAM=MIXED COMPS=CO2 H2O C5H10  
 &  
 NC5H12 C6H12 NC6H14 C7H14 C7H16-1 C8H16 C8H18-1 &  
 C9H18-3 C9H20-1 C10H20-5 C10H22-1 OXHC OXH2O FRACS=0. &  
 0. 0.87258 0.9404 1. 1. 1. 1. 1. 1. 1. 1. 1. 1. &  
 0.48 0.  
 FLASH-SPECS 203S11 TEMP=100. PRES=50. NPHASE=1 &  
 FREE-WATER=NO PHASE=V  
 FLASH-SPECS 203S12 TEMP=100. PRES=50.  
 FLASH-SPECS 203S13 TEMP=100. PRES=50.  
 FLASH-SPECS 203S14 TEMP=100. PRES=50.  
 FLASH-SPECS 203S15 TEMP=100. PRES=50.  
 BLOCK-OPTION FREE-WATER=NO  
  
 BLOCK P201H1 HEATER  
 PARAM TEMP=675. PRES=-5.  
  
 BLOCK P201H2 HEATER  
 PARAM TEMP=300. PRES=-10.  
  
 BLOCK P203H1 HEATER  
 PARAM TEMP=150. PRES=250.  
  
 BLOCK P203H2 HEATER  
 PARAM TEMP=200. PRES=85.  
 BLOCK-OPTION FREE-WATER=YES  
  
 BLOCK P202S FLASH2  
 PARAM TEMP=300. PRES=300.  
  
 BLOCK P203S2 FLASH2



```

PARAM PRES=85. DUTY=0.

BLOCK P203S3 FLASH2
  PARAM TEMP=0. PRES=250.

BLOCK P201A REQUIL
  PARAM NREAC=1 PRES=-15. DUTY=0. NPHASE=1 PHASE=V &
  CHEM-MAXIT=100 MAXIT=100
  STOIC 1 CO -1. * / H2O -1. * / H2 1. * / CO2 1. *
  TAPP-SPEC 1 50.

BLOCK P202C COMPR
  PARAM TYPE=ASME-POLYTROP PRES=450. PEFF=0.85 MEFF=1. &
  NPHASE=1
  BLOCK-OPTION FREE-WATER=NO

BLOCK P202FT USER2
  PARAM NINT=4 NREAL=3 &
  EXCEL-FILE="\GIBSON\HOME FOLDER\LUXB\THESIS\P202FT.XLS'
& NCHAR=4
  INT VALUE-LIST=0 1 0 0
  REAL VALUE-LIST=0. 523. 450.
  CHAR CHAR-LIST="1-IRON 2-COBALT 3-RUTHENIUM 4-NICKEL" &
  "Temperature K" "Pressure Psi"
  FLASH-SPECS 202S2 TP TEMP=400. PRES=350. NPHASE=2 &
  FREE-WATER=YES

DESIGN-SPEC DS-1
  DEFINE CO MOLE-FLOW STREAM=201S2 SUBSTREAM=MIXED &
  COMPONENT=CO
  DEFINE H2 MOLE-FLOW STREAM=201S2 SUBSTREAM=MIXED &
  COMPONENT=H2
F  RATIO=H2/CO
  SPEC "RATIO" TO "1.9"
  TOL-SPEC "0.05"
  VARY STREAM-VAR STREAM=STEAM SUBSTREAM=MIXED &
  VARIABLE=MOLE-FLOW
  LIMITS "30000" "120000"

EO-CONV-OPTI

CALCULATOR C-1
  DEFINE PRES BLOCK-VAR BLOCK=P202C VARIABLE=PRES &

```

```

SENTENCE=PARAM
DEFINE PRESFT BLOCK-VAR BLOCK=P202FT VARIABLE=VALUE-
LIST &
SENTENCE=REAL ELEMENT=3
F PRES=PRESFT
EXECUTE FIRST

STREAM-REPOR MOLEFLOW MASSFLOW MOLEFRAC MASSFRAC &
PROPERTIES=GASPROPS

PROPERTY-REP PCES NOPARAM-PLUS

```

**C. MS Excel spreadsheets incorporated in the user-defined model (P202FT) – Base Case**

In this Excel spreadsheet, data is divided into four distinct tables. Each table is on its own sheet. The sheet and the corresponding table have the same name. The data in Aspen\_Input Sheet are calculated by ASPEN PLUS and then loaded by the ASPEN PLUS and MS Excel spreadsheet interface. Data in Aspen\_Output Sheet are calculated by the Calculation Sheet with the user input Integer parameters and Real parameters.

**Aspen\_IntParams Sheet**

| INTPARAMS |   | Description |            |
|-----------|---|-------------|------------|
| 1         | 0 | Iron        | User Input |
| 2         | 1 | Cobalt      | User Input |
| 3         | 0 | Ruthenium   | User Input |
| 4         | 0 | Nickel      | User Input |

**Aspen\_RealParams Sheet**

| REALPARAMS |     | Description   |            |
|------------|-----|---------------|------------|
| 1          | 0   | Future Use    | User Input |
| 2          | 523 | Temperature K | User Input |
| 3          | 450 | Pressure Psi  | User Input |

## Aspen\_Input Sheet

| INPUT    | 202S1       |
|----------|-------------|
| H2       | 14.16623381 |
| N2       | 0.068600234 |
| CO       | 7.474706456 |
| CO2      | 0.07568414  |
| H2O      | 1.014323962 |
| CH4      | 7.76589E-05 |
| C2H4     | 0           |
| C2H6     | 0           |
| C3H6     | 0           |
| C3H8     | 0           |
| NC4H8    | 0           |
| NC4H10   | 0           |
| C5H10    | 0           |
| NC5H12   | 0           |
| C6H12    | 0           |
| NC6H14   | 0           |
| C7H14    | 0           |
| C7H16-1  | 0           |
| C8H16    | 0           |
| C8H18-1  | 0           |
| C9H18-3  | 0           |
| C9H20-1  | 0           |
| C10H20-5 | 0           |
| C10H22-1 | 0           |
| C11H22-2 | 0           |
| C11H24   | 0           |
| C12H24-2 | 0           |
| C12H26   | 0           |
| C13H26-2 | 0           |
| C13H28   | 0           |
| C14H28-2 | 0           |
| C14H30   | 0           |
| C15H30-2 | 0           |
| C15H32   | 0           |
| C16H32-2 | 0           |
| C16H34   | 0           |
| C17H34   | 0           |
| C17H36   | 0           |
| C18H36-1 | 0           |
| C18H38   | 0           |

## Aspen\_Output Sheet

| OUTPUT   | 202S2      |
|----------|------------|
| H2       | 2.81730282 |
| N2       | 0.06860023 |
| CO       | 1.80024096 |
| CO2      | 0.07568414 |
| H2O      | 6.68878945 |
| CH4      | 0.63922507 |
| C2H4     | 0.0069619  |
| C2H6     | 0.00433013 |
| C3H6     | 0.03248887 |
| C3H8     | 0.02066913 |
| NC4H8    | 0.03654998 |
| NC4H10   | 0.02352158 |
| C5H10    | 0.04987438 |
| NC5H12   | 0.03232062 |
| C6H12    | 0.04089698 |
| NC6H14   | 0.02662689 |
| C7H14    | 0.03353551 |
| C7H16-1  | 0.02190725 |
| C8H16    | 0.0274991  |
| C8H18-1  | 0.01800922 |
| C9H18-3  | 0.02254926 |
| C9H20-1  | 0.01479657 |
| C10H20-5 | 0.01849038 |
| C10H22-1 | 0.01215228 |
| C11H22-2 | 0.01516211 |
| C11H24   | 0.00997772 |
| C12H24-2 | 0.01243292 |
| C12H26   | 0.00819053 |
| C13H26-2 | 0.01019499 |
| C13H28   | 0.00672235 |
| C14H28-2 | 0.00835989 |
| C14H30   | 0.00551663 |
| C15H30-2 | 0.00685511 |
| C15H32   | 0.0045267  |
| C16H32-2 | 0.00562119 |
| C16H34   | 0.0037141  |
| C17H34   | 0.00460937 |
| C17H36   | 0.00304715 |
| C18H36-1 | 0.00377968 |
| C18H38   | 0.00249983 |

|   |              |
|---|--------------|
| C19H38  | 0            |
| C19H40  | 0            |
| C20H40  | 0            |
| C20H42  | 0            |
| OXVAP   | 0            |
| OXHC  | 0            |
| OXH2O   | 0            |
| C10AP   | 0            |
| C21OP   | 0            |
| C22OP   | 0            |
| C23OP   | 0            |
| C24OP   | 0            |
| C25OP   | 0            |
| C26OP   | 0            |
| C27OP   | 0            |
| C28OP   | 0            |
| C29OP   | 0            |
| C30WAX  | 0            |
| TOTFLOW   | 22.79962626  |
| TEMP  | 601.3697615  |
| PRES  | 3102640.785  |
| ENTHALPY  | -3425975.844 |
| VAP FRAC  | 1            |
| LIQ FRAC  | 0            |
| ENTROPY   | 2313.635951  |
| DENSITY   | 7.045723841  |
| MOLE WT   | 11.4674194   |
| * Properties of the Stream 202S1 loaded by Aspen Plus |              |

|  |            |
|--|------------|
| C19H38   | 0.00309934 |
| C19H40   | 0.00205071 |
| C20H40   | 0.00254146 |
| C20H42   | 0.00168222 |
| OXVAP  | 0.0023161  |
| OXHC   | 0.01094046 |
| OXH2O  | 0.00776651 |
| C10AP  | 0          |
| C21OP  | 0.00346621 |
| C22OP  | 0.00284255 |
| C23OP  | 0.00233109 |
| C24OP  | 0.00191164 |
| C25OP  | 0.00156766 |
| C26OP  | 0.00128556 |
| C27OP  | 0.00105423 |
| C28OP  | 0.00086456 |
| C29OP  | 0.00070893 |
| C30WAX   | 0.00212049 |
| TOTFLOW  | 12.6927827 |
| TEMP   | 0          |
| PRES   | 0          |
| ENTHALPY   | 0          |
| VAP FRAC   | 0          |
| LIQ FRAC   | 0          |
| ENTROPY  | 0          |
| DENSITY  | 0          |
| MOLE WT  | 0          |
| * Properties of the Stream 202S2 calculated by Calculation Sheet |            |

### Calculation Sheet

1. Calculate the chain growth probability  $\alpha$  of each catalyst type and CO conversion fraction using the two Real Parameters input: Temperature and Pressure. Then calculate the  $\alpha$  of the specified catalysts with Integer Parameters input. The olefin fraction is a constant of 0.6.

| CONVERSION of CO |             | OLEFIN FRACTION |           |            |  |
|------------------|-------------|-----------------|-----------|------------|--|
| 0.75915563       | F(T,P)      | 0.6             | Constant  |            |  |
| Alpha=           | Fe          | Cobalt          | Ruthenium | Nickel     |  |
| 0.819999672      | 0.913107823 | 0.819999672     | 0.8810586 | 0.47685972 |  |
|                  | F1(T,P)     | F2(T,P)         | F3(T,P)   | F4(T,P)    |  |

2. Calculate the mass flow of the hydrocarbons produced in F-T synthesis using data from the Aspen-Input Sheet and the conversion fraction of CO calculated in Table 1.

|     | H2          | CO          | H2O         | Total        |          |
|-----|-------------|-------------|-------------|--------------|----------|
| IN  | 14.16623381 | 7.474706456 | 1.014323962 |              | Kmol/sec |
|     | 28.55629411 | 209.3695177 | 18.27324904 | 259.5299047  | Kg/sec   |
| OUT | 2.817302823 | 1.800240964 | 6.688789454 | 11.45061762  | Kmol/sec |
|     | 5.679119032 | 50.4254695  | 120.4998798 | 179.9353122  | Kg/sec   |
|     |             |             |             | Hydrocarbons |          |
| DIF | 11.34893098 | 5.674465492 | -5.67446549 |              | Kmol/sec |
|     | 22.69786197 | 158.8850338 | -102.140379 | 79.59459256  | Kg/sec   |

3. Calculate the WT% of hydrocarbons with carbon number from 4 to 29 by the Anderson-Schultz-Flory equation. The WT% of the C<sub>30+</sub> is calculated by a relation  $W_{mn} = (1 - \alpha)(m\alpha^{m-1} - n\alpha^n) + \alpha^m - \alpha^n$  derived from ASF equation, in which  $m=30$  and  $n = \infty$ . C<sub>1</sub>-C<sub>4</sub> WT% and oxygenates WT% are calculated by multiply empirical factors to the amount which is the substrata of 100 and total of C<sub>4</sub> to C<sub>30+</sub>. Then calculate the mass flows by multiply the total hydrocarbon mass flow to each WT%.

| Carbon # | G(N, Alpha) | EXP(G)      | WT%=<br>100*N*EXP(G) | Mass Flow<br>kg/sec |
|----------|-------------|-------------|----------------------|---------------------|
| N        |             |             |                      |                     |
| 1        | -3.42959321 | 0.032400118 | 12.8822649           | 10.25358625         |
| 2        | -3.62804455 | 0.026568086 | 0.4089608            | 0.325510675         |
| 3        | -3.82649589 | 0.021785822 | 2.8627255            | 2.278574723         |
| 4        | -4.02494723 | 0.017864367 | 4.2940883            | 3.417862084         |
| 5        | -4.22339857 | 0.014648775 | 7.3243875            | 5.829816382         |
| 6        | -4.4218499  | 0.012011991 | 7.2071944            | 5.736537024         |
| 7        | -4.62030124 | 0.009849828 | 6.8948799            | 5.487951557         |
| 8        | -4.81875258 | 0.008076856 | 6.4614849            | 5.142992544         |
| 9        | -5.01720392 | 0.006623019 | 5.9607174            | 4.744408724         |
| 10       | -5.21565526 | 0.005430874 | 5.4308737            | 4.322681774         |
| 11       | -5.4141066  | 0.004453315 | 4.8986461            | 3.8990574           |
| 12       | -5.61255794 | 0.003651717 | 4.3820598            | 3.487882679         |
| 13       | -5.81100928 | 0.002994406 | 3.8927283            | 3.098401206         |
| 14       | -6.00946062 | 0.002455412 | 3.4375771            | 2.736125509         |
| 15       | -6.20791195 | 0.002013437 | 3.0201558            | 2.403880735         |
| 16       | -6.40636329 | 0.001651018 | 2.6416286            | 2.102593508         |

|       |             |             |            |             |
|-------|-------------|-------------|------------|-------------|
| 17    | -6.60481463 | 0.001353834 | 2.3015180  | 1.831883861 |
| 18    | -6.80326597 | 0.001110144 | 1.9982583  | 1.590505586 |
| 19    | -7.00171731 | 0.000910317 | 1.7296029  | 1.376670396 |
| 20    | -7.20016865 | 0.00074646  | 1.4929198  | 1.188283445 |
| 21    | -7.39861999 | 0.000612097 | 1.2854034  | 1.023111637 |
| 22    | -7.59707133 | 0.000501919 | 1.1042223  | 0.878901264 |
| 23    | -7.79552267 | 0.000411574 | 0.9466193  | 0.753457782 |
| 24    | -7.993974   | 0.00033749  | 0.8099765  | 0.644697531 |
| 25    | -8.19242534 | 0.000276742 | 0.6918547  | 0.550678921 |
| 26    | -8.39087668 | 0.000226928 | 0.5900134  | 0.469618796 |
| 27    | -8.58932802 | 0.000186081 | 0.5024189  | 0.399898307 |
| 28    | -8.78777936 | 0.000152586 | 0.4272420  | 0.340061535 |
| 29    | -8.9862307  | 0.000125121 | 0.3628504  | 0.288809288 |
| 30+   |             |             | 1.9786365  | 1.574887636 |
| OXVAP |             |             | 0.1481742  | 0.11793865  |
| OXHC  |             |             | 1.1853936  | 0.943509202 |
| OXH2O |             |             | 0.4445226  | 0.353815951 |
|       |             |             | 28.3021750 | 79.59459256 |

4. Calculated every component mass and mole flows using the data got in the above table and the constant of olefin fraction. The molecular weights of every component in the Table are the same as those used in ASPEN PLUS to calculate the mole flows from mass flows. A program of Micro in Excel copies the mole flows to the Aspen\_Output Sheet and then loaded into Stream 202S2.

|         | MOLE FLOW   | MASS FLOW   | MW       |
|---------|-------------|-------------|----------|
| CH4     | 0.63922507  | 10.2548321  | 16.0426  |
| C2H4    | 0.006961902 | 0.195306405 | 28.0536  |
| C2H6    | 0.004330125 | 0.13020427  | 30.0694  |
| C3H6    | 0.032488874 | 1.367144834 | 42.0804  |
| C3H8    | 0.020669125 | 0.911429889 | 44.0962  |
| NC4H8   | 0.036549984 | 2.050717251 | 56.1072  |
| NC4H10  | 0.023521581 | 1.367144834 | 58.123   |
| C5H10   | 0.049874381 | 3.497889829 | 70.134   |
| NC5H12  | 0.032320624 | 2.331926553 | 72.1498  |
| C6H12   | 0.040896976 | 3.441922215 | 84.1608  |
| NC6H14  | 0.02662689  | 2.29461481  | 86.1766  |
| C7H14   | 0.033535507 | 3.292770934 | 98.1876  |
| C7H16-1 | 0.021907247 | 2.195180623 | 100.2034 |
| C8H16   | 0.027499105 | 3.085795527 | 112.2144 |
| C8H18-1 | 0.018009222 | 2.057197018 | 114.2302 |
| C9H18-3 | 0.022549257 | 2.846645234 | 126.2412 |

|          |             |             |             |
|----------|-------------|-------------|-------------|
| C9H20-1  | 0.014796569 | 1.897763489 | 128.257     |
| C10H20-5 | 0.018490383 | 2.593609064 | 140.268     |
| C10H22-1 | 0.012152281 | 1.72907271  | 142.2838    |
| C11H22-2 | 0.015162108 | 2.33943444  | 154.2948    |
| C11H24   | 0.009977717 | 1.55962296  | 156.3106    |
| C12H24-2 | 0.012432924 | 2.092729607 | 168.3216    |
| C12H26   | 0.008190527 | 1.395153071 | 170.3374    |
| C13H26-2 | 0.010194993 | 1.859040724 | 182.3484    |
| C13H28   | 0.006722349 | 1.239360483 | 184.3642    |
| C14H28-2 | 0.008359891 | 1.641675305 | 196.3752    |
| C14H30   | 0.005516632 | 1.094450204 | 198.391     |
| C15H30-2 | 0.006855108 | 1.442328441 | 210.402     |
| C15H32   | 0.004526703 | 0.961552294 | 212.4178    |
| C16H32-2 | 0.005621186 | 1.261556105 | 224.4288    |
| C16H34   | 0.003714098 | 0.841037403 | 226.4446    |
| C17H34   | 0.004609371 | 1.099130317 | 238.4556    |
| C17H36   | 0.003047155 | 0.732753544 | 240.4714    |
| C18H36-1 | 0.003779683 | 0.954303352 | 252.4824    |
| C18H38   | 0.00249983  | 0.636202235 | 254.4982    |
| C19H38   | 0.003099339 | 0.826002237 | 266.5092    |
| C19H40   | 0.002050715 | 0.550668158 | 268.525     |
| C20H40   | 0.002541457 | 0.712970067 | 280.536     |
| C20H42   | 0.001682217 | 0.475313378 | 282.5518    |
| C21OP    | 0.003466207 | 1.023111637 | 295.1675    |
| C22OP    | 0.002842553 | 0.878901264 | 309.1943    |
| C23OP    | 0.002331091 | 0.753457782 | 323.2211    |
| C24OP    | 0.001911643 | 0.644697531 | 337.2479    |
| C25OP    | 0.001567659 | 0.550678921 | 351.2747    |
| C26OP    | 0.001285565 | 0.469618796 | 365.3015    |
| C27OP    | 0.001054227 | 0.399898307 | 379.3283    |
| C28OP    | 0.000864559 | 0.340061535 | 393.3351    |
| C29OP    | 0.000708927 | 0.288809288 | 407.3891    |
| C30WAX   | 0.002120492 | 1.574887636 | 742.6992    |
| OXVAP    | 0.002316096 | 0.11793865  | 50.92131    |
| OXHC     | 0.010940459 | 0.943509202 | 86.24037    |
| OXH2O    | 0.007766505 | 0.353815951 | 45.55665    |
| TOTAL    | 12.6927827  | 79.59583842 | 79.59583842 |

### Aspen Plus and MS Excel Spreadsheet Interface Source Code

'Global to hold the current block id. Set in AspenStartIteration, and  
'cleared in AspenEndIteration.



```
Dim g_blockId As String
```

```
Public Function AspenCalculate() As String
```

```
'Called to solve the model for the given inputs. Called after writing out all of the  
input data.
```

```
'By default we just call Calculate. If you are writing VBA code to solve your  
model call it from here.
```

```
Calculate
```

```
AspenCalculate = ""
```

```
'Range("aspen_output").Value = 20.5
```

```
'AspenCalculate = "This is an error in calc"
```

```
End Function
```

```
Public Function AspenStartIteration(blockId As String) As String
```

```
'Called at the start of each iteration of the model, before the model  
'gets calculated.
```

```
g_blockId = blockId
```

```
AspenStartIteration = ""
```

```
End Function
```

```
Public Function AspenEndIteration() As String
```

```
'Called at the end of each iteration of the model, after the model has been  
calculated.
```

```
'If you want to save the last table of data to a uniquely named sheet, this would be  
the place to do it.
```

```
'The following line will create a sheet called Aspen_Output_B2, if the block id is  
B2, and copy all of
```

```
'the data currently held in the Aspen_Output sheet.
```

```
CopySheetForBlock "Output", g_blockId
```

```
AspenEndIteration = ""
```

```
End Function
```

```
Public Function AspenEndRun(runid As String)
```

```
'Called when the Aspen Plus engine is quitting, after all blocks have been  
processed. The runid is
```

```
'passed from the engine. You may want to use the runid as part of the filename if  
saving the sheet at the
```

```
'end of a run.
```

```
'To save at the end of a run comment out the following
```

```
ThisWorkbook.Save
```

```
AspenEndRun = ""
```



End Function

Private Function GetSheet(sheetName As String) As Worksheet

'Create the sheet if it is not already there.

On Error Resume Next

Set GetSheet = Nothing

Set GetSheet = Worksheets(sheetName)

If Err = 9 Then 'subscript out of range

Err.Clear

On Error GoTo 0

Set GetSheet = Worksheets.Add

GetSheet.Name = sheetName

End If

End Function

Private Sub CopySheetForBlock(sheetNameToCopy As String, blockName As String)

Dim sheetNameForBlock As String

Dim sheetToCopy As Worksheet

Dim sheetForBlock As Worksheet

Set sheetToCopy = Worksheets("Aspen\_" & sheetNameToCopy)

sheetNameForBlock = "Aspen\_" & sheetNameToCopy & "\_" & blockName

Set sheetForBlock = GetSheet(sheetNameForBlock)

sheetToCopy.UsedRange.Copy

sheetForBlock.Range("A1").PasteSpecial Paste:=xlPasteValues

End Sub

Public Function ahtest() As Integer

Dim testSheet As Worksheet

Set testSheet = GetSheet("Aspen\_TestMacros")

testSheet.Cells.Clear

' Write out all the counts

testSheet.Cells(1, 1).Value = "Number of Input Streams:"

testSheet.Cells(1, 2).Value = ahNumStreams([aspen\_input])

testSheet.Cells(2, 1).Value = "Number of Output Streams:"

testSheet.Cells(2, 2).Value = ahNumStreams([Aspen\_Output])

testSheet.Cells(3, 1).Value = "Number of Components:"

testSheet.Cells(3, 2).Value = ahNumComps([aspen\_input])

```

testSheet.Cells(4, 1).Value = "Number of Integer Parameters:"
testSheet.Cells(4, 2).Value = ahNumParams([Aspen_IntParams])

testSheet.Cells(5, 1).Value = "Number of Real Parameters:"
testSheet.Cells(5, 2).Value = ahNumParams([Aspen_RealParams])

' Write out all the input stream data
Dim rowNum As Integer
rowNum = 7
Dim n As Integer
For n = 1 To ahNumStreams([aspen_input])
    testSheet.Cells(rowNum, n + 1).Value = ahStreamName([aspen_input], n)
Next n

For n = 1 To ahNumComps([aspen_input])
    testSheet.Cells(rowNum + n, 1).Value = ahCompName([aspen_input], n)
Next n

n = 8 + ahNumComps([aspen_input])
testSheet.Cells(n, 1).Value = "FLOW"
testSheet.Cells(n + 1, 1).Value = "TEMP"
testSheet.Cells(n + 2, 1).Value = "PRES"

Dim i As Integer
Dim j As Integer

For i = 1 To ahNumStreams([aspen_input])
    For j = 1 To ahNumComps([aspen_input])
        testSheet.Cells(rowNum + j, i + 1).Value = ahGetValue([aspen_input], j, i)
    Next j
Next i

n = 8 + ahNumComps([aspen_input])

For i = 1 To ahNumStreams([aspen_input])
    testSheet.Cells(n, i + 1).Value = ahGetValue([aspen_input], j, i)
    testSheet.Cells(n + 1, i + 1).Value = ahGetValue([aspen_input], j + 1, i)
    testSheet.Cells(n + 2, i + 1).Value = ahGetValue([aspen_input], j + 2, i)
Next i

test = 1
End Function

```

```

Public Function ahGetValue(r As Range, row As Variant, Optional col As Variant)
As Variant
If VarType(row) = vbString Then
    row = FindRowFromHeader(r, row)
End If
If IsMissing(col) Then
    col = 1
ElseIf VarType(col) = vbString Then
    col = FindColFromHeader(r, col)
End If
ahGetValue = r.Cells(row, col)
End Function
Public Sub ahSetValue(r As Range, row As Variant, col As Variant, vNewValue
As Variant)
If VarType(row) = vbString Then
    row = FindRowFromHeader(r, row)
End If
If VarType(col) = vbString Then
    col = FindColFromHeader(r, col)
End If
r.Cells(row, col) = vNewValue
End Sub
Public Function FindRowFromHeader(r As Range, row As Variant)
FindRowFromHeader = 0
With r
    Dim i As Integer
    For i = 1 To .rows.Count
        If .Cells(i, 0).Value = row Then
            FindRowFromHeader = i
            Exit For
        End If
    Next i
End With
End Function
Public Function FindColFromHeader(r As Range, col As Variant)
FindColFromHeader = 0
With r
    Dim i As Integer
    For i = 1 To .Columns.Count
        If .Cells(0, i).Value = col Then
            FindColFromHeader = i
            Exit For
        End If
    Next i
End With
End Function

```

```
Next i
End With
End Function
```

```
Public Function ahCompName(r As Range, compNum As Integer) As String
ahCompName = r.Cells(compNum, 0)
End Function
Public Function ahStreamName(r As Range, streamNum As Integer) As String
ahStreamName = r.Cells(0, streamNum)
End Function
```

```
Public Function ahNumParams(r As Range) As Integer
ahNumParams = r.rows.Count
End Function
Public Function ahNumStreams(r As Range) As Integer
ahNumStreams = r.Columns.Count
End Function
Public Function ahNumComps(r As Range) As Integer
ahNumComps = r.rows.Count - 9
End Function
```